

See discussions, stats, and author profiles for this publication at: <https://www.researchgate.net/publication/278031234>

Bis(ether-functionalized NHC) Nickel(II) Complexes, Trans to Cis Isomerization Triggered by Water Coordination, and Catalytic Ethylene Oligomerization

ARTICLE *in* ORGANOMETALLICS · JUNE 2015

Impact Factor: 4.13 · DOI: 10.1021/om5008506

CITATION

1

READS

47

5 AUTHORS, INCLUDING:



Sophie Hameury

University of Strasbourg

7 PUBLICATIONS 43 CITATIONS

SEE PROFILE



Pierre de Frémont

University of Strasbourg

35 PUBLICATIONS 1,946 CITATIONS

SEE PROFILE



Pierre-Alain R. Breuil

IFP Energies nouvelles

26 PUBLICATIONS 224 CITATIONS

SEE PROFILE



Pierre Braunstein

University of Strasbourg

634 PUBLICATIONS 12,518 CITATIONS

SEE PROFILE

Bis(ether-functionalized NHC) Nickel(II) Complexes, *Trans* to *Cis* Isomerization Triggered by Water Coordination, and Catalytic Ethylene Oligomerization

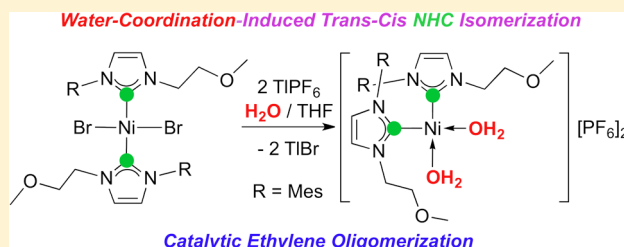
Sophie Hameury,[†] Pierre de Frémont,[†] Pierre-Alain R. Breuil,[‡] Hélène Olivier-Bourbigou,[‡] and Pierre Braunstein^{*,†}

[†]Laboratoire de Chimie de Coordination, Institut de Chimie (UMR 7177 CNRS), Université de Strasbourg, 4 Rue Blaise Pascal, CS 90032, 67081 Strasbourg, France

[‡]IFP Energies nouvelles, Rond-Point de l'échangeur de Solaize, BP3, 69360 Solaize, France

Supporting Information

ABSTRACT: The new nickel(II) complexes containing NHC ligands N-substituted by a CH₂CH₂OR ether group (R = Me or Ph) [NiCl₂{ImMes(C₂OMe)}₂] (6), [NiCl₂{Im*n*-Bu(C₂OMe)}₂] (7), [NiBr₂{ImDiPP(C₂OMe)}₂] (8), [NiBr₂{ImMes(C₂OMe)}₂] (9), [NiBr₂{Im*n*-Bu(C₂OMe)}₂] (10), NiBr₂{ImMes(C₂OPh)}₂ (18), [NiI₂{ImDiPP(C₂OMe)}₂] (21), [NiI₂{ImMes(C₂OMe)}₂] (22), and [NiI₂{Im*n*-Bu(C₂OMe)}₂] (23) were synthesized in good yields and fully characterized by NMR spectroscopy and X-ray diffraction analysis. The reaction conditions were optimized and further applied to thioether or nonfunctionalized NHC ligands, affording [NiBr₂{ImDiPP(C₂SPh)}₂] (19) and [NiBr₂{ImDiPP(*n*-Bu)}₂] (20), respectively. Equilibria involving *syn/anti* isomers were unveiled for complexes [NiCl₂{ImDiPP(C₂OMe)}₂] (5), 6–10, and 18–23. Reactions of 6 and 20 with a halide abstractor afforded the dicationic aquo complexes *cis*-[Ni{ImMes(C₂OMe)}₂(H₂O)₂][PF₆]₂ (27) and *cis*-[Ni{ImDiPP(*n*-Bu)}₂(H₂O)₂][PF₆]₂ (28), in which a *cis* arrangement of the carbene ligands is evidenced, which contrasts with that in their precursors. These molecules represent rare examples of nickel aquo NHC complexes and of complexes with two *cis* monodentate NHC ligands. The new complexes reported in this work (15 crystal structures) displayed moderate activities as precatalysts for ethylene oligomerization and favored dimerization.



INTRODUCTION

N-Heterocyclic carbenes (NHCs) have been increasingly studied over the last 20 years, and their strong σ -electron-donating properties usually lead to very stable bonding to late transition metals.¹ This is a prerequisite for further ligand-controlled reactivity, and the resulting complexes often display remarkable catalytic activity owing to their resistance against temperature, air, and moisture.^{1d,2} In many instances, this makes NHC complexes even more attractive than their phosphine counterparts.^{2,3} Recent developments in the field of hybrid ligands consisting in the association of one (or more) NHC(s) with a neutral or an anionic donor group have shown a beneficial effect for the stabilization of reactive species and for the formation of polynuclear motifs.^{3b,4}

In the field of catalytic olefin oligomerization mediated by NHC complexes, chromium chemistry is prevalent⁵ since the development by McGuinness and co-workers of highly active Cr(III) complexes, where the catalytic cycle involves metalacyclic intermediates.^{5c,d} Only a few examples of oligomerization catalysts of alkynes or alkenes based on NHC ruthenium(II),⁶ nickel(II),⁷ zirconium(IV),⁸ rhodium(I),⁹ or palladium(II)¹⁰ complexes have been reported. In this regard, the still limited number of publications dealing with NHC nickel(II)

catalysts is staggering when compared to the considerable amount of literature dedicated to Ni(II) complexes with other types of ligands (e.g., phosphines, diimines, imino-pyridines, phosphino-enolates) well known to promote ethylene oligomerization.¹¹ Indeed, since the discovery of the “nickel effect”,¹² considerable efforts have been devoted to the synthesis of nickel-based catalysts, and a prominent example of industrial success in nickel-catalyzed ethylene oligomerization is the Shell Higher Olefin Process (SHOP), which involves an anionic P,O ligand.^{11a,g,l,13}

Nickel(II) complexes with nonfunctionalized NHC ligands have already been evaluated in ethylene oligomerization and found to be selective for dimerization, with low to moderate activities.^{7a–d} In most cases, the authors point out the facile reductive elimination of the NHC ligand, which results in catalyst deactivation.¹⁴ Various strategies have been suggested to reduce this deactivation pathway: (i) the use of ionic liquids as solvent and imidazolium salt pool, to compensate for any

Special Issue: Mike Lappert Memorial Issue

Received: August 21, 2014

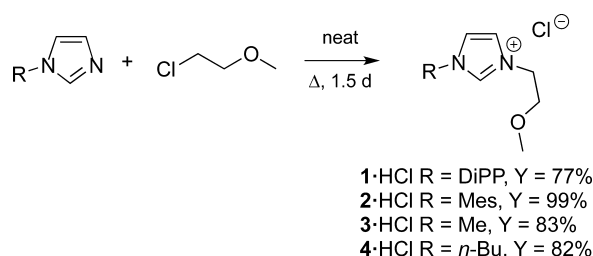
Published: October 21, 2014

reductive elimination occurring at the nickel center, the large excess of imidazolium salts allowing rapid regeneration of the catalyst by oxidative addition,^{7a} and (ii) the addition of a second donor group to firmly anchor the metal in the vicinity of the carbene donor site. Following the latter approach, some nickel(II) complexes with pyridine-, salicylaldiminato-, ether-, enolate-, alcoholate-, and aryloxy-functionalized NHC ligands have been prepared that catalyze the oligomerization or polymerization of various alkenes (e.g., ethylene, propylene, norbornene, styrene) upon activation.^{7c–g,15} When the donor function attached to the NHC ligand is neutral, its reversible coordination to the metal center can occur, and this hemilabile behavior in solution can result in catalysts with improved properties (equilibrium between stabilized dormant species and highly reactive, coordinatively unsaturated species).¹⁶ In previous work we have studied Ni(II) ethylene oligomerization precatalysts with heterobidentate ligands that facilitate a fine-tuning of their catalytic properties.^{11n,17} More recently, we reported the synthesis and catalytic properties in ethylene oligomerization of Ni(II) complexes with alcohol- and alcoholate-functionalized NHC.^{7f,g} Their sensitivity triggered our interest for Ni(II) complexes with ether-functionalized NHC ligands, potential candidates for hemilabile behavior,¹⁶ and our results are presented in this paper.

RESULTS AND DISCUSSION

Synthesis of the Complexes. Following reaction conditions similar to those used for the synthesis of 1-(2,6-diisopropylphenyl)-3-(2-methoxyethyl)-1*H*-imidazol-3-ium chloride ([ImH]DiPP(C₂OMe))Cl, **1**·HCl, i.e., the quaternization of *N*-substituted imidazoles,^{7f} we prepared 1-mesityl-3-(2-methoxyethyl)-1*H*-imidazol-3-ium chloride ([ImH]Mes(C₂OMe))Cl, **2**·HCl, 1-methyl-3-(2-methoxyethyl)-1*H*-imidazol-3-ium chloride ([ImH]Me(C₂OMe))Cl, **3**·HCl, and 1-*n*-butyl-3-(2-methoxyethyl)-1*H*-imidazol-3-ium chloride ([ImH]*n*-Bu(C₂OMe))Cl, **4**·HCl in good yields (82–99%) (Scheme 1). The ¹H NMR spectra in CD₂Cl₂ of **1**·HCl–**4**·HCl display

Scheme 1. Synthesis of the Imidazolium Salts **1**·HCl–**4**·HCl



the characteristic resonance of the NCHN proton between 9 and 10 ppm, in agreement with the formation of the imidazolium salts.

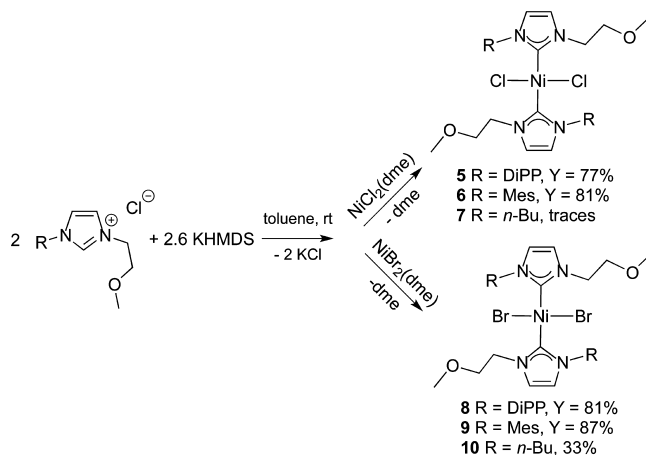
Several ether *N*-functionalized NHC complexes have been reported in the literature with various transition metals; they were synthesized by transmetalation from a precursor NHC Ag(I) complex¹⁸ or by deprotonation of an imidazolium salt with either an external base prior to metalation^{18b,19} or an internal base directly incorporated as a ligand into the precursor metal complex.^{18b,g,19b,e,f,20}

We previously obtained by a transmetalation reaction the Ni(II) complex dichlorobis[1-(2,6-diisopropylphenyl)-3-(2-methoxyethyl)-1*H*-imidazol-2(3*H*)-ylidene]nickel

([NiCl₂{ImDiPP(C₂OMe)}₂], **5**), bearing the ether-functionalized NHC ligand **1**. However, since a yield of only 50% was obtained,^{7f} other synthetic approaches were assessed. In contrast to the straightforward synthesis of [PdCl(acac)-(NHC)]-type complexes, which are obtained by boiling a mixture of imidazolium salts and [Pd(acac)₂] in THF or dioxane,^{19b,23} a similar approach with **1**·HCl and [Ni(acac)₂] was unsuccessful. Hence the direct deprotonation of the imidazolium precursor followed by metal complexation was explored. During their attempts to synthesize ether-functionalized NHCs by deprotonation of the parent imidazolium salts with *n*-BuLi, Dixneuf *et al.* noticed the formation of vinyl-functionalized NHCs, resulting from LiOMe elimination.²¹ Thus, we explored the use of other bases to perform the deprotonation of the azolium moiety, including Cs₂CO₃, NEt₃, and NaH with (or without) a catalytic amount of KO^{*t*}-Bu (potassium *tert*-butoxide) or potassium hexamethyldisilazane (KHMDs). Our best results were obtained with KHMDs, most likely because its reduced nucleophilicity prevented attack on the ether function and formation of a vinyl-functionalized NHC. The deprotonation of the imidazolium salt was followed by the addition of [NiX₂(dme)] (X = Cl or Br, dme = dimethoxyethane) to form the corresponding [NiX₂(NHC)₂] complex without the need to isolate the sensitive free carbene (Scheme 2).

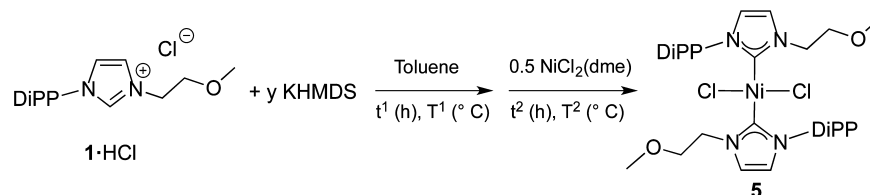
Scheme 2. Synthesis of the Complexes

[NiCl₂{ImDiPP(C₂OMe)}₂] (**5**),^{7f}
 [NiCl₂{ImMes(C₂OMe)}₂] (**6**), [NiCl₂{Im*n*-Bu(C₂OMe)}₂]
 (**7**), [NiBr₂{ImDiPP(C₂OMe)}₂] (**8**),
 [NiBr₂{ImMes(C₂OMe)}₂] (**9**), and [NiBr₂{Im*n*-
 Bu(C₂OMe)}₂] (**10**)



The complexes **5**, dichlorobis[1-mesityl-3-(2-methoxyethyl)-1*H*-imidazol-2(3*H*)-ylidene]nickel ([NiCl₂{ImMes(C₂OMe)}₂], **6**), dichlorobis[1-butyl-3-(2-methoxyethyl)-1*H*-imidazol-2(3*H*)-ylidene]nickel ([NiCl₂{Im*n*-Bu(C₂OMe)}₂], **7**), dibromobis[1-(2,6-diisopropylphenyl)-3-(2-methoxyethyl)-1*H*-imidazol-2(3*H*)-ylidene]nickel ([NiBr₂{ImDiPP(C₂OMe)}₂], **8**), dibromobis[1-mesityl-3-(2-methoxyethyl)-1*H*-imidazol-2(3*H*)-ylidene]nickel ([NiBr₂{ImMes(C₂OMe)}₂], **9**), and dibromobis[1-butyl-3-(2-methoxyethyl)-1*H*-imidazol-2(3*H*)-ylidene]nickel ([NiBr₂{Im*n*-Bu(C₂OMe)}₂], **10**) were isolated using this method as orange (chlorido complexes) or orange-red powders (bromido complexes) (Scheme 2). All complexes are soluble in THF,

Scheme 3. Optimization of the Reaction Conditions for the Synthesis of 5



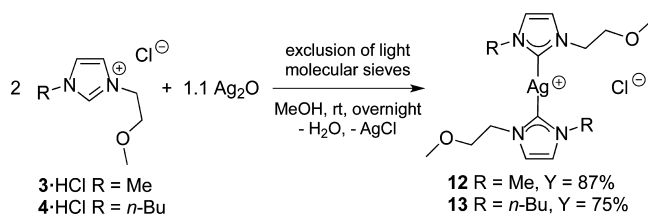
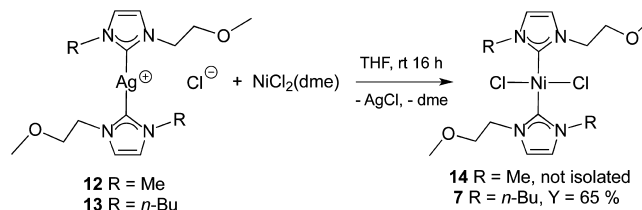
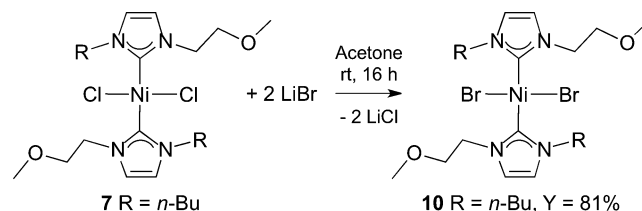
benzene, or acetone and insoluble in ether, hexane, pentane, or water.

A screening of the reaction conditions (reaction time, temperature, relative stoichiometry metal precursor/base/imidazolium salt) performed with **5** allowed their optimization (Scheme 3 and Table 1).

Table 1. Optimization of the Reaction Conditions for the Synthesis of **5**

<i>y</i>	<i>t</i> ¹ (h)	<i>T</i> ¹ (°C)	<i>t</i> ² (h)	<i>T</i> ² (°C)	yield (%)
1	18	−78	3	−78	59
1	2.5	RT	16	RT	61
1.5	1	RT	3	RT	not clean
1.3	1	RT	3	RT	77

No improvement of the yield was observed when KHMDS was added to a toluene suspension of the imidazolium salt at −78 °C or at room temperature. The stoichiometry of the base was adjusted, and a slight excess (1.3 equiv) with respect to the imidazolium salt led to an improved yield. Addition of a larger excess of base (1.5 equiv) resulted in the formation of paramagnetic byproduct(s) that could not be readily separated from **5**. Finally, the reaction times were decreased to 2 h for the deprotonation and 3 h for the complexation without affecting the yield (Scheme 2). After the reaction mixture was filtered through Celite, the toluene solution was evaporated to dryness to afford orange or red powders of the complexes (for X = Cl or Br, respectively), which were purified by precipitation from their THF solution with pentane and further trituration of the resulting solids with pentane. For additional purification, the resulting powders were washed with H₂O and solubilized in toluene, the solution was dried with Na₂SO₄, and the product was precipitated by addition of pentane, yielding **5**, **6**, **8**, and **9** in 77–87% yield, whereas lower yields were observed for **7** and **10**. Purification of **5**, **6**, **8**, and **9** was performed without the need for anhydrous conditions, whereas **7** and **10** proved to be moisture-sensitive. Therefore, purification of the complexes with water was not possible for **7** and **10**, which limited their initial yields, and this led us to modify the synthetic strategy to improve the yields (see Schemes 4–6). This method involving carbene transmetalation was also applied to pro-ligand **3·HCl**

Scheme 4. Synthesis of the Ag(I) Complexes **12** and **13**Scheme 5. Transmetalation Reactions Affording **7**Scheme 6. Synthesis of **10** by Halide Metathesis

since insoluble product(s) were initially observed when applying the conditions of Scheme 2 (see below).

The formation of the diamagnetic complexes **5–10** was confirmed by ¹H NMR spectroscopy with the complete disappearance of the characteristic signals of the imidazolium salts. Furthermore, in the ¹³C{¹H} NMR spectra, the signals for the carbenes between 169.8 and 171.5 ppm for **5–7** and between 171.1 and 172.6 ppm for **8–10** are consistent with the formation of [NiX₂(NHC)₂] complexes.²² Similarly to previous observations with **5**,^{7f} two products were observed by NMR spectroscopy to be in equilibrium for **5–10**. Detailed NMR studies will be discussed below. The mass spectra of complexes **5**, **6**, and **8** display only one signal for *m/z* = [NiX(NHC)₂]⁺. The mass spectrum of **7** contains only two signals, for *m/z* = [NiX(NHC)₂]⁺ and *m/z* = [(NHC)H]⁺, whereas for **9** and **10** numerous unassigned fragments are generated even though the signal accounting for *m/z* = [NiX(NHC)₂]⁺ is the most intense.

The structures of complexes **6** and **7** were unambiguously determined by X-ray diffraction analysis of orange crystals grown by stratification of THF solutions of the complexes with pentane (Figure 1, Table 2). These structures are similar to that reported previously for complex **5**.^{7f}

Complex **6** crystallizes in the triclinic system with the *P* $\bar{1}$ space group, and complex **7** in the monoclinic system with the *P*2₁/*c* space group. The Ni(II) centers are positioned on inversion centers in **7**. Two isomers are present in the crystal structure of **7**, and this point will be discussed below. All the complexes display similar connectivities, with a square planar coordination geometry around the Ni(II) centers, which are ligated by two mutually *trans* monodentate NHC ligands and two terminal chlorides. The Ni–C_{carbene} and Ni–Cl bond distances are in the range 1.903(3)–1.917(3) Å and 2.1733(8)–2.1882(8) Å, respectively (Table 2). The C_{carbene}–

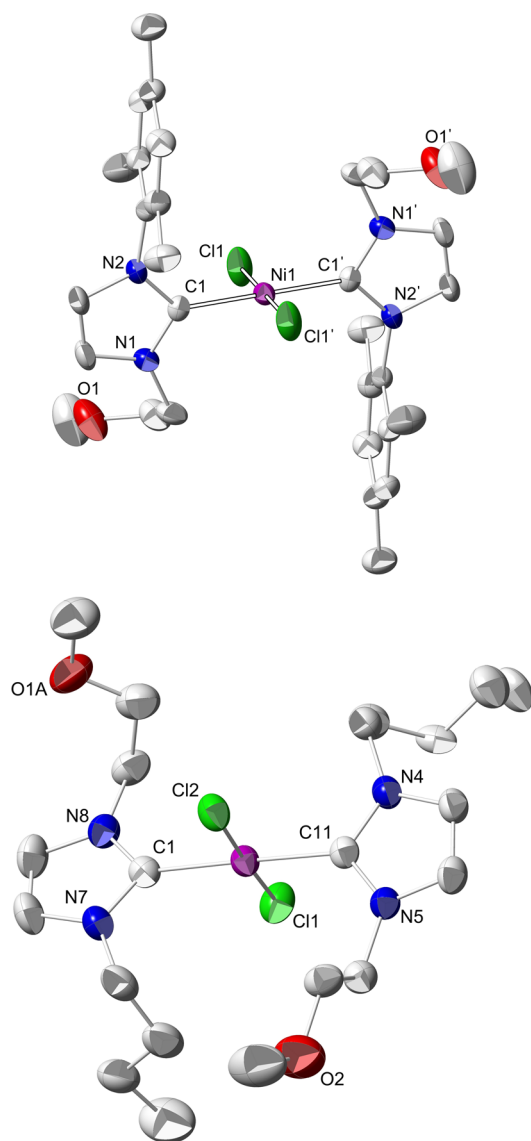


Figure 1. ORTEP of the molecular structure of $[\text{NiCl}_2\{\text{ImMes}(\text{C}_2\text{OMe})\}_2]$ (**6**) (top) and $[\text{NiCl}_2\{\text{Im}n\text{-Bu}(\text{C}_2\text{OMe})\}_2]$ (**7**) (bottom, only one isomer was chosen; see below). Ellipsoids are set at the 30% probability level. Hydrogen atoms have been omitted for clarity.

$\text{Ni}-\text{C}_{\text{carbene}}$ and $\text{Cl}-\text{Ni}-\text{Cl}$ bond angles are between $176.9(1)-180^\circ$ and $176.56(3)-180^\circ$, respectively. These values are in good agreement with those reported for similar $[\text{NiCl}_2(\text{NHC})_2]$ complexes.^{7f,g,22a,b,e,f}

For comparison, the dibromido complexes **8–10**, which are analogous to **5–7**, respectively, were also prepared (Scheme 2), and their structures were established by single-crystal X-ray diffraction (Table 2). The $\text{Ni}(\text{II})$ centers display a square planar coordination environment with $\text{C}_{\text{carbene}}-\text{Ni}-\text{C}_{\text{carbene}}$ and $\text{Br}-\text{Ni}-\text{Br}$ angles in the range $179.7(4)-180^\circ$ and $179.55(6)-180^\circ$, respectively. The $\text{Ni}-\text{C}_{\text{carbene}}$ and $\text{Ni}-\text{Br}$ bond distances are in the range $1.894(7)-1.914(4)$ and $2.280(1)-2.3257(8)$ Å, respectively. All these values are in good agreement with metrical data for similar $[\text{NiBr}_2(\text{NHC})_2]$ complexes.^{22b,e,f,i} More details are provided in the SI.

A few blue crystals of an unexpected byproduct of the synthesis of **5** were obtained once by slow evaporation of the crude reaction mixture in toluene. Their nature and structure were established unambiguously by X-ray diffraction analysis to

Table 2. Selected Bond Distances in $\text{Ni}(\text{II})$ Complexes

complex	X	$\text{Ni}-\text{C}_{\text{carbene}}$ (Å)	$\text{Ni}-\text{X}$ (Å)
5	Cl	1.910(2)	2.1828(8)
		1.902(2)	2.1822(8)
6	Cl	1.916(3)	2.1733(8)
		1.903(3)	2.1859(7)
7	Cl	1.915(3)	2.1849(8)
		1.917(3)	2.1882(8)
8	Br	1.894(7)	2.288(1)
		1.895(7)	2.280(1)
9	Br	1.914(4)	2.3004(6)
		1.911(4)	2.3174(4)
10	Br	1.911(4)	2.3199(4)
		1.905(4)	2.3257(8)
18	Br	1.912(3)	2.3023(8)
		1.915(3)	2.3313(8)
19	Br	1.914(2)	2.3186(2)
		1.906(4)	2.3155(4)
20	Br	1.911(3)	2.5000(3)
		1.916(3)	2.4982(3)
21	I	1.910(4)	2.5025(6)
		1.916(4)	2.5393(6)
22	I	1.912(4)	2.5174(3)
		1.912(4)	2.5174(3)

correspond to the salt $[(\text{ImH})\text{DiPP}(\text{C}_2\text{OMe})][\text{NiCl}_3\{\text{ImDiPP}(\text{C}_2\text{OMe})\}]$ (**11**) (Figure 2).

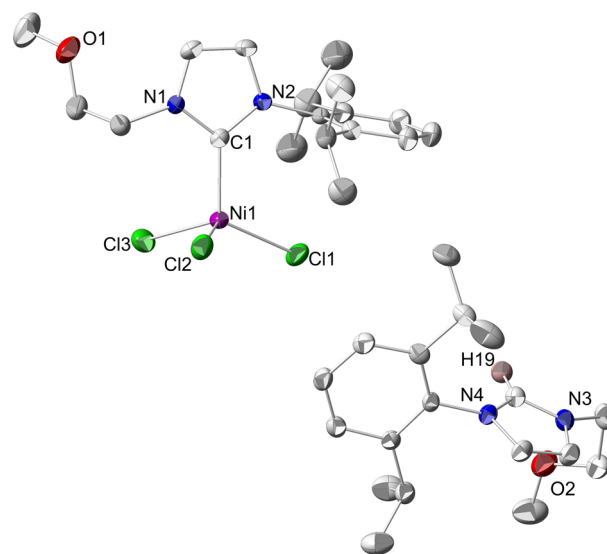


Figure 2. ORTEP of the molecular structure of **11** in $11 \cdot \text{C}_7\text{H}_8$. Ellipsoids are set at the 30% probability level. Hydrogen atoms have been omitted for clarity, except the NCHN hydrogen.

Compound **11** crystallizes in the triclinic system with the $P\bar{1}$ space group. A molecule of toluene has cocrystallized with **11**. The $\text{Ni}(\text{II})$ center displays a slightly distorted tetrahedral coordination geometry and is surrounded by a monodentate NHC ligand and three terminal chlorides. The $\text{C}_{\text{carbene}}-\text{Ni}-\text{Cl}$ and $\text{Cl}-\text{Ni}-\text{Cl}$ bond angles range from $102.80(1)^\circ$ to $113.5(1)^\circ$ and from $107.77(5)^\circ$ to $113.85(5)^\circ$, respectively. The $\text{Ni}-\text{C}_{\text{carbene}}$ bond distance is equal to $1.981(4)$ Å, and the $\text{Ni}-\text{Cl}$ bond distances are in the range $2.234(1)-2.279(1)$ Å. The electroneutrality of **11** is ensured by the presence of the corresponding imidazolium cation $[(\text{ImH})\text{DiPP}(\text{C}_2\text{OMe})]^+$. To the best of our knowledge, **11** is the first example of a

Scheme 7. Attempted Synthesis of 11

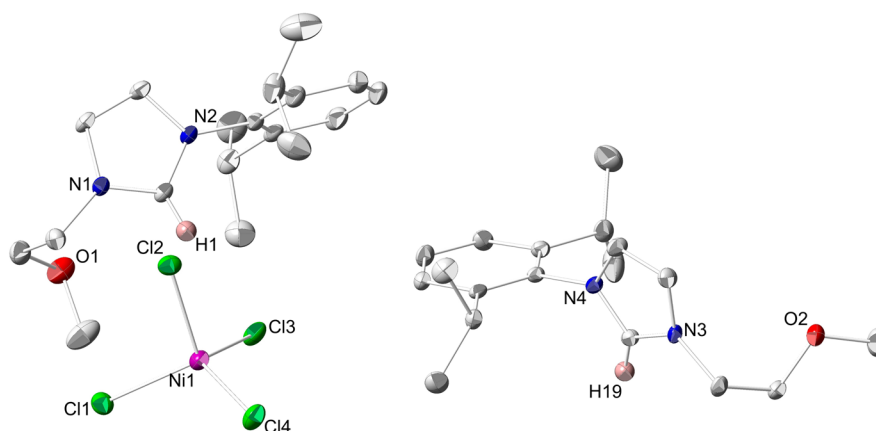
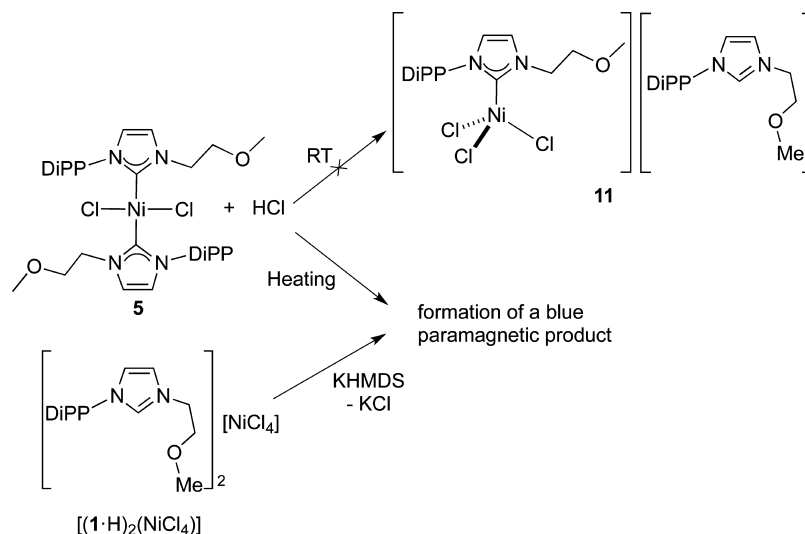


Figure 3. ORTEP of the molecular structure of $[(1\cdot H)_2(NiCl_4)]$. Ellipsoids are set at the 30% probability level. Hydrogen atoms have been omitted for clarity, except the NCHN hydrogen atoms.

complex with the formula $[NiX_3(NHC)]^-$, although such anions are commonly observed with phosphines.²³

Attempts to selectively synthesize **11** by reaction of **5**, in toluene, with 1 or 20 equiv of HCl to favor the protonation of the carbene ligand and its replacement by a chloride were unsuccessful at room temperature. A slight reactivity was observed at 115 °C with 2 equiv of HCl, resulting in the formation of a blue paramagnetic precipitate (Scheme 7). Once dissolved, the precipitate did not produce any suitable crystals for X-ray diffraction, and no further characterizations were undertaken. In the presence of HCl, the Ni–C_{carbene} bond of an alkyl chelate revealed to be resistant,²⁴ whereas a similar Ni–C_{carbene} bond from an alcoholate chelate was cleaved at room temperature.^{7g} From these results, it is clear that the stability, under acidic conditions, of NHC–Ni complexes is challenging to rationalize. The synthesis of **11** was then attempted by reacting the imidazolium salt $[(ImH)DiPP(C_2OMe)_2][NiCl_4]$ $[(1\cdot H)_2(NiCl_4)]$ with 1 equiv of KHMDS. An uncharacterized blue paramagnetic precipitate was formed, and no direct proof of the formation of **11** could be obtained (Scheme 7). Prior to this reaction, the salt $[(1\cdot H)_2(NiCl_4)]$ was isolated in good yield (see Experimental Section). It is soluble in acetone, THF, and CH_2Cl_2 and insoluble in Et_2O , pentane, or hexane. Suitable crystals for X-ray diffraction analysis were grown by

stratification of a THF solution of $[(1\cdot H)_2(NiCl_4)]$ with diethyl ether (Figure 3).

The compound $[(1\cdot H)_2(NiCl_4)]$ crystallizes in the monoclinic system with the $P2_1/c$ space group. The $[NiCl_4]^{2-}$ dianion displays the expected tetrahedral coordination geometry. In the imidazolium moieties, the N–C bond lengths and the N–C–N angles range from 1.329(4) to 1.333(4) Å and 108.6(3)° to 108.5(3)°, respectively. These values are consistent with those reported for other imidazolium salts.²⁵ We recently observed a similar structure with an alcohol-functionalized imidazolium salt.^{7g}

As mentioned above, the methodology providing the ether-functionalized $[NiX_2(NHC)_2]$ complexes **5/6** and **8/9** in high yields (from 77% to 87%) with *N*-aryl substituents was not efficient with the *N*-*n*-Bu substituent, since only 33% of the desired complex **10** and traces of **7** were obtained. Since both **7** and **10** are water-sensitive, it was not possible to purify them by washing the solid mixture with H_2O . Furthermore, with *R* = Me as *N*-substituent, formation of an insoluble product was observed. For these complexes, we decided to apply the well-known transmetalation method from Ag(I) complexes.

The silver(I) complexes bis[1-(2-methoxyethyl)-3-methyl-1*H*-imidazol-2(3*H*)-ylidene]silver(I) chloride ($[Ag\{ImMe(C_2OMe)_2\}_2]Cl$, **12**) and bis[1-*n*-butyl-3-(2-methoxyethyl)-

1*H*-imidazol-2(3*H*)-ylidene]silver(I) chloride ([Ag{Im*n*-Bu(C₂OMe)}₂]Cl, **13**) were isolated as white or beige powders in 87% and 75% yields, respectively, by reacting overnight 2 equiv of the imidazolium salt **3**·HCl or **4**·HCl with 1.1 equiv of Ag₂O in methanol under the exclusion of light (Scheme 4). The resulting complexes **12** and **13** displayed similar solubilities (THF, acetone, CH₂Cl₂). Although they are stable toward light for a few days, they should best be stored for prolonged periods under the exclusion of light.

The formation of complexes **12** and **13** was confirmed by ¹H NMR spectroscopy with the complete disappearance of the characteristic NCHN signal of the imidazolium salts, indicating their deprotonation. The ¹³C{¹H} NMR signal of the carbene carbons appears at 183.3 and 180.8 ppm for **12** and **13**, respectively. No coupling with ^{107/109}Ag was observed, in contrast to analogous Ag(I) complexes with alcohol-functionalized NHCs.^{7f} The mass spectra of complexes **12** and **13** display only two signals for *m/z* = [Ag(NHC)₂]⁺ and [(NHC)H]⁺, which indicates partial reprotonation of the carbene ligand under the analysis conditions (no imidazolium signal was visible in the ¹H NMR spectra).

Despite several attempts, no single crystal was obtained for **13**, whereas suitable crystals for X-ray diffraction analysis were obtained by stratification of a concentrated solution of **12** in CH₂Cl₂ with diethyl ether. The structure of **12** was unambiguously determined using X-ray diffraction analysis (Figure 4).

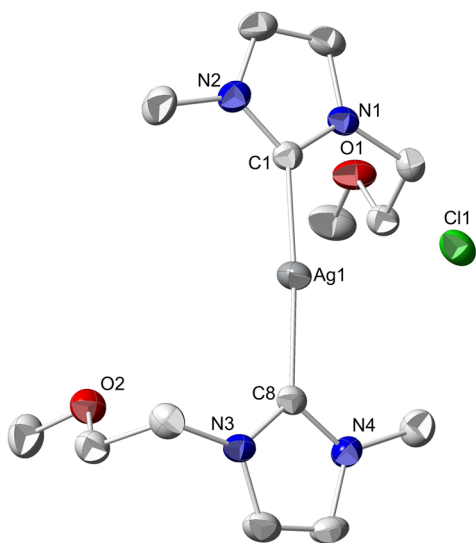


Figure 4. ORTEP of the molecular structure of [Ag{ImMe(C₂OH)}₂]Cl (**12**). Ellipsoids are set at the 30% probability level. Hydrogen atoms have been omitted for clarity.

Complex **12** crystallizes in the triclinic system with the $P\bar{1}$ space group. The Ag(I) center displays a nearly linear coordination environment with two coordinated NHC ligands and a C_{carbene}–Ag–C_{carbene} angle equal to 168.2(1)°. The Ag–C_{carbene} distances of 2.100(3) and 2.113(3) Å are in good agreement with other distances reported for homoleptic cationic bis(NHC) silver(I) complexes.²⁶ The structure of **12** reveals a weak electrostatic interaction between the silver cation and the chloride ion (Ag–Cl distance of 3.0525(8) Å), as observed in related complexes.^{7f,22d,27} The chloride is only acting as a counteranion for the [Ag(NHC)₂]⁺ moiety. A similar complex featuring the same connectivity of Ag(I) with ligand **3** but containing [AgCl₂][−] as anion was published in 2011.^{20h}

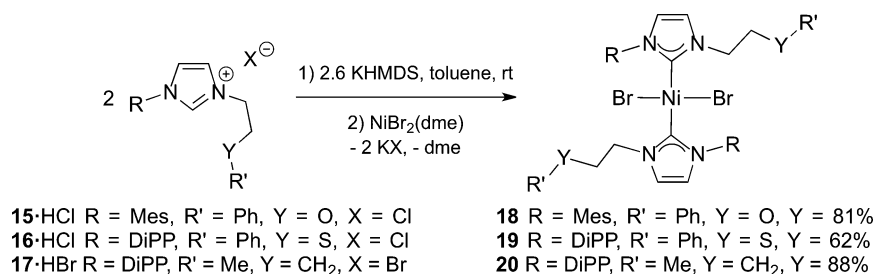
A transmetalation reaction to Ni(II) was performed using [NiCl₂(dme)] as metallic precursor in THF (Scheme 5). With R = Me as N-substituent, the product formed featured a very low solubility, similarly to what was observed when KHMDS was used for the deprotonation of the imidazolium cation. This prevented separation from the AgCl formed and its full characterization. However, when R = *n*-Bu, the desired complex **7** was selectively obtained in reasonable yield (65%). NHC transmetalation thus appears preferable to deprotonation of the imidazolium precursor.

In order to obtain the complex [NiBr₂(NHC)₂] (**10**), an anion metathesis reaction was performed on **7** with LiBr (Scheme 6). The corresponding reaction with KBr was unsuccessful, likely for solubility reasons. Complex **10** was obtained in 81% yield.

As stated in the Introduction, the additional donor group tethered to the NHC moiety may interact in solution with the metal center and affect its reactivity. Therefore, modifications of the stereoelectronic properties of the N-functional group, i.e., by changing the nature of the heteroatom (O *vs* S or C) or the hydrocarbon group directly linked to it (Me *vs* Ph) may influence the catalytic properties of the resulting Ni(II) complexes. For this reason, 1-(2,6-diisopropylphenyl)-3-(2-phenoxyethyl)-1*H*-imidazol-3-ium chloride ([ImH]DiPP-(C₂OPh)]Cl, **15**·HCl) was synthesized using the same procedure as for the imidazolium salts **1**·HCl–**4**·HCl (Scheme 1). Its thioether analogue 1-(2,6-diisopropylphenyl)-3-(2-(phenylthio)ethyl)-1*H*-imidazol-3-ium chloride ([ImH]DiPP-(C₂SPh)]Cl, **16**·HCl) was obtained in good yield via a slightly modified procedure compared to that leading to *N*-alkyl-*N'*-thioether imidazolium chlorides²⁸ or *N*-aryl-*N'*-thioether imidazolium iodides.²⁹ Quaternization of the *N*-substituted imidazole with 2-chloroethyl phenyl sulfide afforded **16**·HCl in 72% yield.

The scope of the methodology used for the synthesis of the [NiX₂(NHC)₂] complexes was then explored (Scheme 8). The

Scheme 8. Synthesis of Complexes 18–20



size of the ether moiety was increased, using a OPh group instead of OMe, without any detrimental effect on the yields of the reactions, and dibromobis[1-mesityl-3-(2-phenoxyethyl)-1*H*-imidazol-2(3*H*)-ylidene]nickel ($[\text{NiBr}_2\{\text{ImMes}(\text{C}_2\text{OPh})\}_2]$, **18**) was isolated in 81% yield. Even though the yield decreased to 62% with a thioether group, the same methodology could be applied to the synthesis of dibromobis[1-(2,6-diisopropylphenyl)-3-(2-(phenylthio)ethyl)-1*H*-imidazol-2(3*H*)-ylidene]nickel ($[\text{NiBr}_2\{\text{ImDiPP}(\text{C}_2\text{SPh})\}_2]$, **19**). To allow comparison of their catalytic properties (see below), the complex dibromobis[1-butyl-3-(2,6-diisopropylphenyl)-1*H*-imidazol-2(3*H*)-ylidene]nickel ($[\text{NiBr}_2\{\text{ImDiPP}(n\text{-Bu})\}_2]$, **20**) containing a *N*-*n*-Bu substituent instead of the ether group was prepared in 88% yield starting from the known 1-(2,6-diisopropylphenyl)-3-(*n*-butyl)-1*H*-imidazol-3-ium bromide ($[(\text{ImH})\text{DiPP}(n\text{-Bu})]\text{Br}$, **17**·HBr).³⁰ All complexes featured similar properties (color, solubility, and stability) compared to **9** and **10**. A closely related thioether-functionalized NHC ligand was previously coordinated to Ni(II) in 2007 by Labande *et al.* using similar reaction conditions.^{22c}

The formation of the complexes **18–20** was confirmed by ¹H NMR spectroscopy with the complete disappearance of the characteristic NCHN signal of the imidazolium precursor. Consistent with the formation of $[\text{NiBr}_2(\text{NHC})_2]$ complexes,²² their carbene signal appears between 171.6 and 172.8 in the ¹³C{¹H} NMR spectra. Two products were again observed by NMR spectroscopy (see below). The mass spectra of complexes **18–20** display minor signals for $m/z = [\text{NiBr}(\text{NHC})_2]^+$, the major signals being for unassigned decomposition products.

Red-orange crystals suitable for X-ray diffraction analysis were grown by stratification of THF solutions of complexes **18–20** with pentane (for **18** and **19**) or ether (for **20**). The molecular structures of **18–20** are depicted in Figure 5.

Complex **18** crystallizes in the triclinic system with the $P\bar{1}$ space group. Complexes **19** and **20** crystallize in the monoclinic system with a $P2_1/c$ space group. The Ni(II) centers are positioned on inversion centers in **19** and **20**. In the complexes, Ni(II) centers in **18–20** display a slightly distorted square planar coordination geometry with $\text{C}_{\text{carbene}}\text{--Ni--C}_{\text{carbene}}$ and Br--Ni--Br bond angles in the range 178.9(1)–180° and 176.97(2)–180°, respectively. Each nickel is surrounded by two NHC ligands in a *trans* arrangement and by two terminal bromides. The Ni– $\text{C}_{\text{carbene}}$ and Ni–Br bond distances are in the range 1.906(4)–1.915(3) and 2.3023(8)–2.3313(8) Å, respectively (Table 2). All these values are in good agreement with those reported for similar $[\text{NiBr}_2(\text{NHC})_2]$ complexes.^{22b,c,f,i}

The chlorido ligands in complexes **5–7** were replaced with iodides, by metathetical exchange using KI in acetone, to form dark purple powders of diiodobis[1-(2,6-diisopropylphenyl)-3-(2-methoxyethyl)-1*H*-imidazol-2(3*H*)-ylidene]nickel ($[\text{NiI}_2\{\text{ImDiPP}(\text{C}_2\text{OMe})\}_2]$, **21**), diiodobis[1-mesityl-3-(2-methoxyethyl)-1*H*-imidazol-2(3*H*)-ylidene]nickel ($[\text{NiI}_2\{\text{ImMes}(\text{C}_2\text{OMe})\}_2]$, **22**), and diiodobis[1-butyl-3-(2-methoxyethyl)-1*H*-imidazol-2(3*H*)-ylidene]nickel ($[\text{NiI}_2\{\text{ImDiPP}(n\text{-Bu})\}_2]$, **23**) with excellent yields (91–99%) (Scheme 9). Complexes **21–23** displayed similar properties (solubility and stability) to their dichlorido or dibromido analogues. The ¹³C{¹H} NMR data indicated the completion of the metathesis reaction since the chemical shifts of the $\text{C}_{\text{carbene}}$ signals were shifted (from 169.8–171.5 ppm to 174.5–175.7 ppm), consistent with the formation of $[\text{NiI}_2(\text{NHC})_2]$ complexes.³¹ After only 3 h

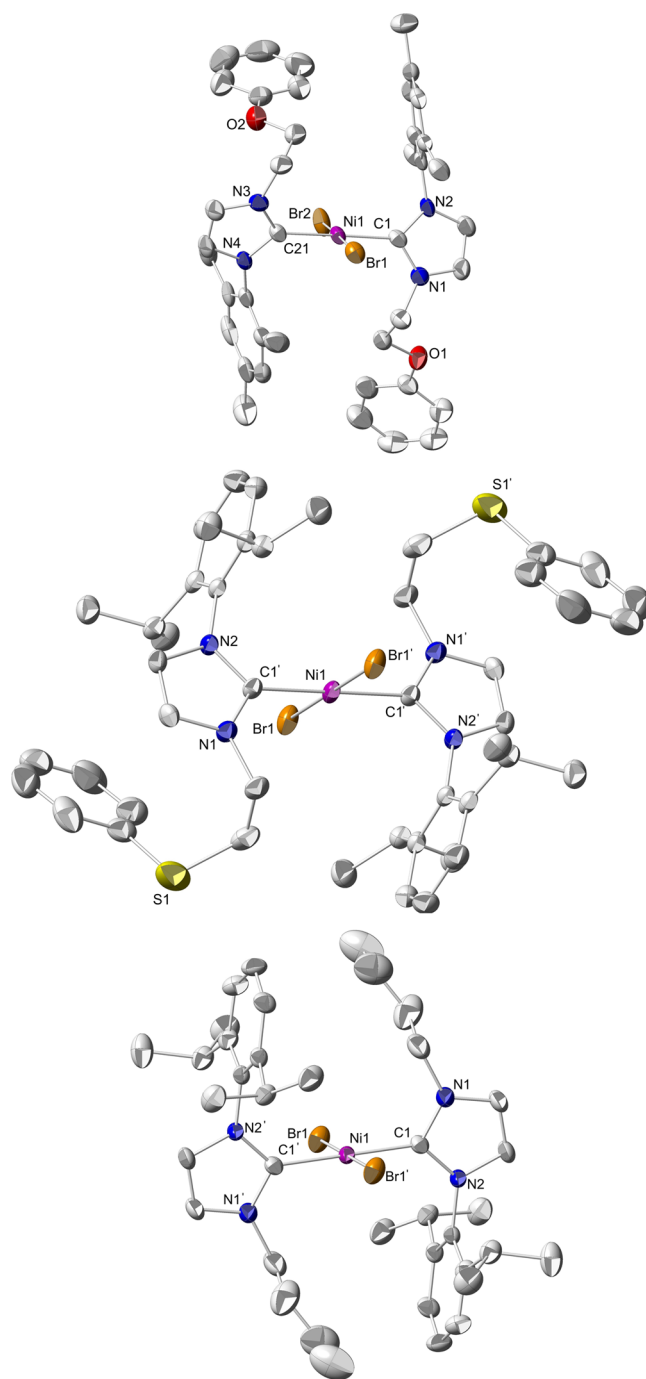
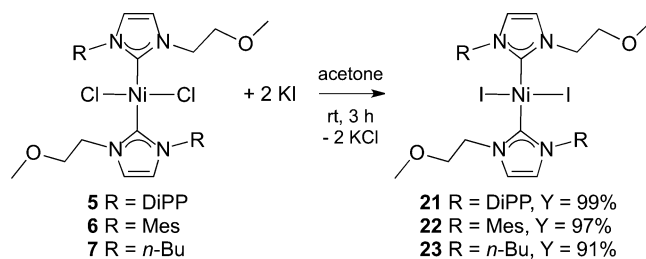
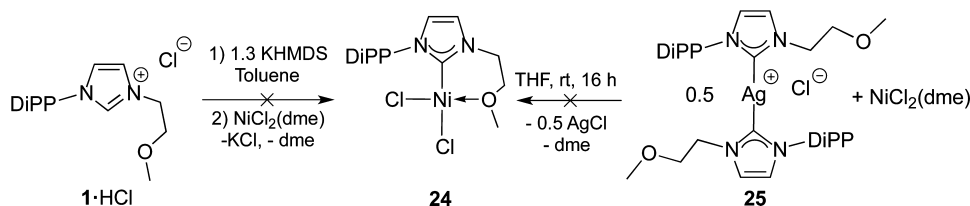


Figure 5. ORTEP of the molecular structures of $[\text{NiBr}_2\{\text{ImMes}(\text{C}_2\text{OPh})\}_2]$ (**18**) (top), $[\text{NiBr}_2\{\text{ImDiPP}(\text{C}_2\text{SPh})\}_2]$ (**19**) (middle), and $[\text{NiBr}_2\{\text{ImDiPP}(n\text{-Bu})\}_2]$ (**20**) (bottom). Ellipsoids are set at the 30% probability level. Hydrogen atoms have been omitted for clarity.

Scheme 9. Synthesis of Complexes **21–23**



Scheme 10. Attempts to Synthesize 24



reaction time at room temperature, no trace of the dichlorido complexes was observed. The mass spectra of complexes **21**–**23** display several signals including that for $m/z = [\text{Ni}(\text{NHC})_2]^+$.

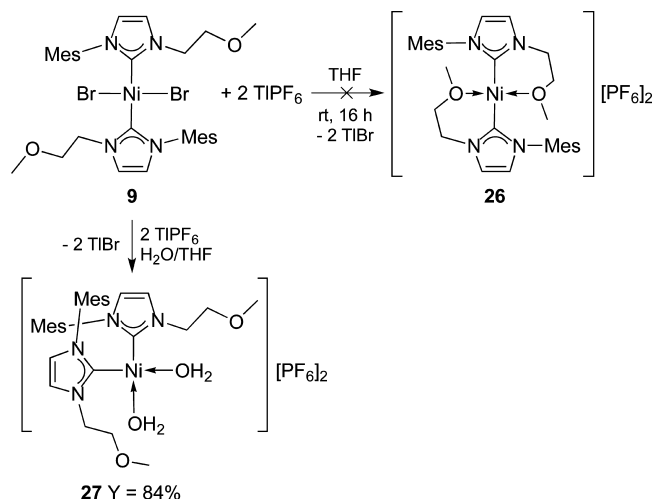
Orange crystals of **21**–**23** suitable for X-ray diffraction were grown by stratification of THF solutions of the complexes with pentane, and their molecular structures were determined (Table 2). They display square planar coordination geometries with $\text{C}_{\text{carbene}}\text{--Ni--C}_{\text{carbene}}$ and I--Ni--I bond angles ranging from $179.5(2)^\circ$ to 180° and from $179.16(6)^\circ$ to 180° , respectively. The $\text{Ni--C}_{\text{carbene}}$ and Ni--I bond distances are between $1.910(4)$ and $1.916(4)$ Å and between $2.4982(3)$ and $2.5393(6)$ Å, respectively. These values are in good agreement with data reported for similar $[\text{Ni}_2(\text{NHC})_2]$ complexes.^{31b,c,32} More details are provided in the SI.

Since no interaction between the metal and the ether function was observed with the various halides, R groups, or ether substituents R' employed, two different strategies were elaborated to favor the chelation of the ether moiety in a complex such as (hypothetical) $[\text{NiCl}_2\{\text{ImDiPP}(\text{C}_2\text{OMe})\}]$ (**24**). First, the coordination of only one NHC ligand to nickel was considered (Scheme 10). Reaction of 1 equiv of free carbene **1**, generated *in situ* using KHMDS, with 1 equiv of $[\text{NiCl}_2(\text{dme})]$, led only to the formation of the bis-NHC complex **5**. Similarly, the reaction of 1 equiv of $[\text{NiCl}_2(\text{dme})]$ with 0.5 equiv of the silver complex **25** (previously described as a transmetalation agent for the synthesis of **5** with a 1:1 ratio)^{7f} provided the exclusive formation of the bis-carbene complex **5**. Whereas Ni(II) chelate complexes comprising a bidentate NHC ligand have been easily prepared using this strategy,^{22e,h,33} the formation of the mono-NHC Ni(II) complex **24** was not possible, in agreement with the well-documented preferential formation of bis-NHC rather than mono-NHC complexes.^{15c,d,34}

Since it was not possible to obtain the mono-NHC complex **24**, the coordination of both ether arms was envisaged to provide the dicationic complex $[\text{Ni}\{\text{ImMes}(\text{C}_2\text{OMe})\}_2][\text{PF}_6]_2$ (**26**) from the precursor bis-NHC complex **9** (Scheme 11). Attempts to abstract the halide ligands from **9** led to decomposition and/or formation of paramagnetic mixtures with AgBF_4 , while NaBF_4 was unreactive. Gratifyingly, a clean reaction occurred with TIPF_6 .

The diastereotopicity of the NCH_2 and CH_2OMe protons,³⁵ evidenced in the ^1H NMR spectrum by the appearance of two multiplets at 4.49–4.39 and 3.49–3.38 ppm and of two multiplets at 3.63–3.53 and 3.18–3.06 ppm, respectively, was suggestive of the coordination of the OMe groups. Moreover, the symmetry of the mesityl group was lost since two singlets for the aromatic CH (instead of one in **9**) and three different signals accounting for the CH_3 protons (instead of two for **9**) were observed. The carbene signal in the ^{13}C NMR spectrum is highly shifted upfield, from 171.1–171.3 ppm to 147.7 ppm, indicating a probable *cis/trans* isomerization. Yellow crystals

Scheme 11. Synthesis of the Bis(aquo) Complex 27



were grown by stratification of an acetone solution of the complex with Et_2O . The structure of the complex obtained was thus determined using X-ray diffraction analysis (Figure 6).

Surprisingly, no coordination of the OMe function was observed, and the bromides were replaced by two water molecules to form $[\text{Ni}\{\text{ImMes}(\text{C}_2\text{OMe})\}_2(\text{H}_2\text{O})_2][\text{PF}_6]_2$ (**27**)

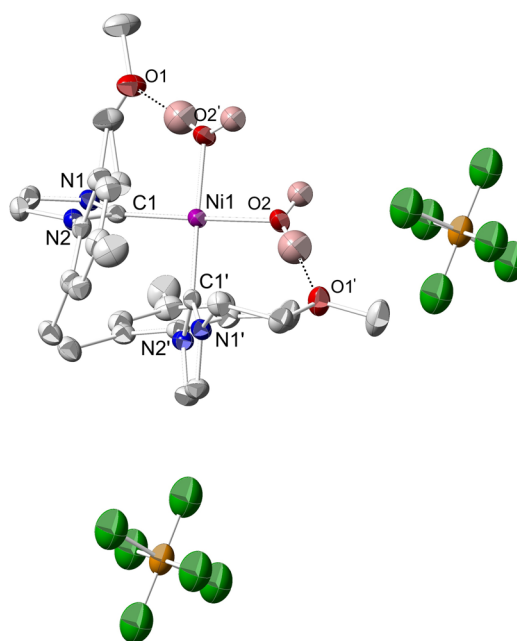


Figure 6. ORTEP of the molecular structure of $[\text{Ni}\{\text{ImMes}(\text{C}_2\text{OMe})\}_2(\text{H}_2\text{O})_2][\text{PF}_6]_2$ (**27**) in $27\cdot\text{Et}_2\text{O}$. Ellipsoids are set at the 30% probability level. Hydrogen atoms have been omitted for clarity, except the H_2O hydrogens.

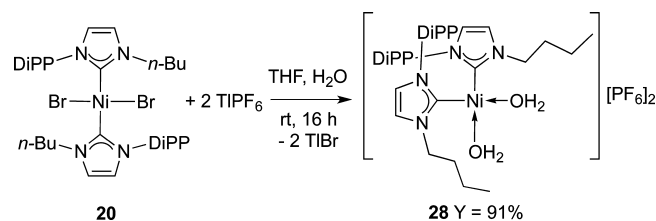
(Scheme 11). The complex **27** cocrystallizes with Et₂O in the monoclinic system with the C2/*c* space group. In the unit cell, the Ni centers are positioned on 2-fold axes. In contrast to their dihalido precursor, the two NHC ligands occupy now mutually *cis* positions. The electroneutrality of the complex is ensured by two PF₆[−] anions that are severely disordered in the crystal lattice. The Ni–C_{carbene} and Ni–OH₂ bond distances are equal to 1.876(5) and 1.907(4) Å, respectively. The Ni(II) centers display a square planar coordination geometry with C_{carbene}–Ni–OH₂ and C_{carbene}–Ni–C_{carbene} bond angles equal to 178.3(2)° and 90.7(3)°, respectively. Interestingly, intramolecular hydrogen bonds are present between the ether moieties and the water molecules (dotted line in Figure 6). The water molecules also interact with the cocrystallized ether via intermolecular hydrogen bonds. To the best of our knowledge, only two examples of aquo NHC nickel complexes have been reported.³⁶ Moreover, except for bischelating NHC ligands, which force the *cis* coordination of the carbene donor groups, examples of nickel complexes with monodentate NHC ligands in *cis* configuration are scarce.^{22i,37} The X-ray data were collected at −40 °C since the crystal shattered at lower temperature. An equilibrium was unveiled using VT NMR spectroscopy, and several species were observed at low temperature (see SI). However, we were not able to characterize them. This equilibrium was reversible upon heating the NMR tube to room temperature. The mass spectrum of complex **27** displays several unassigned signals, but complete displacement of the bromide ligands was evidenced by the fact that no signal displayed the isotopic distribution of Br.

Interestingly, even though no coordination of the ether moiety to Ni(II) was observed in the solid state, the rotation of the functionalized N-substituent was blocked by hydrogen bonding with the H₂O ligands. The diastereotopicity observed in the ¹H NMR spectrum for the NCH₂CH₂OMe signals confirmed the persistence of these hydrogen-bonding interactions in solution.

Despite several attempts, we did not succeed in synthesizing **26**, even with carefully dried solvents. We assume the water is arising from the commercially available TlPF₆. We found that **27** was more conveniently prepared by addition of a few drops of water to the reaction mixture (84% yield). Interestingly, air-stable **27** is insoluble in water, benzene, diethyl ether, hexane, or pentane but soluble in THF or acetone. Surprisingly, when **9** was reacted with TlPF₆ in the presence of nondried methanol, no MeOH coordination was observed, and **27** was observed instead. Moreover, we tried to replace the two water molecules with neutral bidentate ligands such as ethylene glycol or dimethoxyethane, but in each case the formation of a mixture of products was observed. In the presence of 2 equiv of NMe₄Cl (as a chloride source), **27** was converted to the *trans* complex **6**. In contrast to **5**, which is stable toward acids, **27** reacted completely with HCl or HPF₆ and protonation of the NHC was evidenced by ¹H NMR with an imidazolium NCHN resonance, but broadening of the signals prevented further characterization. During the reaction of **27** with HCl, traces of **6** were also observed by ¹H NMR spectroscopy.

For comparison, a similar reaction to that of Scheme 11 was performed with the nonfunctionalized complex [NiBr₂{ImDiPP(*n*-Bu)}₂] (**20**) to see whether the ether moiety was required for the formation of the *cis* isomer (Scheme 12). The ¹H NMR spectrum indicates the formation of a new complex with similar diastereotopicity of the *n*-Bu chains and asymmetry of the DiPP groups. Moreover the carbene signal

Scheme 12. Formation of Complex **28**

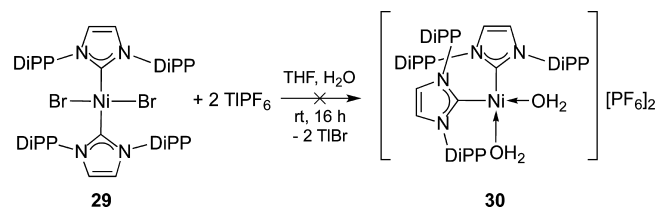


was highly shifted upfield from 171.6–172.6 ppm to 145.0 ppm for **20** and **28**, respectively, supporting a *cis* arrangement of the carbene ligands. The mass spectrum of **28** was not assignable, while the isotopic distribution of each signal indicated the total displacement of the bromido ligands. Complex **28** featured physical properties (color, stability, and solubility) similar to those of its ether-functionalized analogue **27**.

We thus tried to extend the synthetic methodology leading to *cis* complexes to other N-substituents. Surprisingly, the reaction of **8** under conditions similar to those that led to **28** resulted mainly in the reprotonation of the carbene ligand with the minor formation of other unidentified species. When this reaction was attempted with **18**, formation of the desired product was observed concomitant with the formation of another, unidentified complex in a 9:1 ratio (see SI S-25 and S-26 for NMR spectra). Unfortunately, despite several attempts, it was not possible to separate these compounds owing to their similar solubility. The reason(s) for the differences in reactivities between **8** or **18** and **9** or **20** are not yet clear since all complexes featured similar structures and would be expected to possess similar reactivity.

Finally, for comparison, the known symmetrical dibromobis-[1,3-bis(2,6-diisopropylphenyl)-1,3-dihydro-2*H*-imidazol-2-ylidene]nickel, [NiBr₂{Im(DiPP)₂}₂] (**29**), was synthesized according to a published procedure,^{22b} and its reactivity toward TlPF₆ was assessed. Surprisingly, whereas the formation of the *cis* complexes **27** and **28** was efficient upon addition of TlPF₆ to the corresponding [NiBr₂(NHC)₂] complex, no reaction was observed with **29** even upon addition of excess halide abstractor or upon heating (Scheme 13). The steric hindrance of the DiPP substituents may prevent the halide abstraction and disfavor the formation of the *cis* isomer.

Scheme 13. Attempted Formation of Complex **30**



Description of the Equilibrium. Similarly to what was previously observed for complex **5**,^{7f} two sets of NMR signals were obtained for all complexes (**5**–**10** and **18**–**23**), except for **27** and **28**. The presence in the ¹³C{¹H} NMR spectra of two very close signals accounting for a Ni(II)-coordinated C_{carbene} indicates the presence of two NHC Ni complexes, **A** and **B**. The other ¹³C{¹H} NMR signals (for **A/B**) are very close for all species (**5**–**10** and **18**–**23**) and can even overlap (for **7**, **10**, and **23**). For instance with **5**, the observed differences between the chemical shifts assigned to similar carbon atoms in **A** and **B**

never exceeded 1.4 ppm. Two sets of signals were also observed in the ^1H NMR spectra, with very similar chemical shifts except for the protons of the functionalized arms ($\text{CH}_2\text{CH}_2\text{YR}'$) (for **5**, **6**, **8**, **9**, **18**, **19**, **20**, **21**, and **22**). For instance, with **5**, the differences in chemical shifts for the two $\text{CH}_2\text{CH}_2\text{YR}'$ and $\text{CH}_2\text{CH}_2\text{YR}'$ groups were equal to 0.69 and 0.33 ppm, respectively.

Attempts to separate the different species A/B by flash chromatography, washing, or selective precipitation were unsuccessful. Only one of the two species was crystallized for complexes **5**, **6**, **8**, **9**, **18**, **19**, **20**, **21**, **22**, and **23**, despite numerous attempts. Redissolution of authentic crystals (with only one species present in the unit cell), in deuterated solvents, resulted in the re-formation of the A/B mixture in the same ratio. Infrared spectra of the crystals and powders of the complexes did not reveal any difference, in agreement with the existence of only one type of complex in the solid state. Consequently, a dynamic equilibrium in solution was suspected between A and B, and this was further confirmed by a ROESY NMR experiment. The percentage of each species is solvent-dependent, and the amount of the minor species B increases for each complex in acetone- d_6 compared to C_6D_6 (Table 3).

Table 3. Proportion of the Complexes A and B as a Function of the Solvent^a

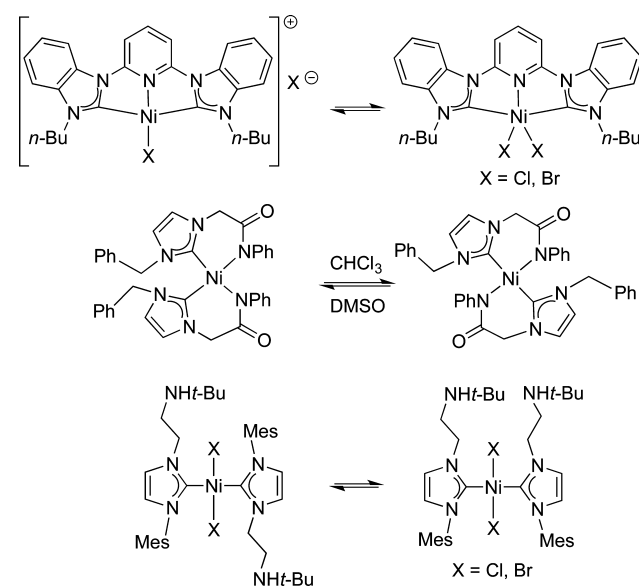
complex	A/B ratio in C_6D_6	A/B ratio in acetone- d_6
5	91/9	82/18
6	74/26	67/33
8	77/23	70/30
9	57/43	50/50
18	57/43	56/44
19	66/34	62/38
20	77/23	75/25
21	35/65	32/68
22	24/76	21/79

^aThe A/B ratio was determined by integration of the ^1H NMR signals.

The sequential addition of acetone- d_6 to a solution of complex in C_6D_6 leads to progressive modification of the A/B ratio, indicating that the equilibrium is solvent-dependent. Note that for **7**, **10**, and **23**, an accurate A/B ratio could not be calculated since the ^1H NMR signals for both A/B species overlap, and roughly 50% of each A and B appear to be present in solution (irrespective of the solvent used). The increase of the A/B ratio is reversible upon evaporation of acetone and redissolution in C_6D_6 , highlighting the reversibility of the dynamic equilibrium. The percentage of B depends on the halide and increases in the sequence $\text{Cl} < \text{Br} < \text{I}$. Surprisingly, for the iodo complexes, species B becomes predominant compared to A. A variable-temperature ^1H NMR study in C_6D_6 revealed that increasing the temperature to 70 °C did not affect the A/B ratio.

Different types of solution equilibria for nickel(II) complexes with functionalized NHC ligands have been reported in the literature (Scheme 14). Brown et al. described the synthesis of a Ni(II) complex bearing a tridentate NHC and a labile halide, with a coordination geometry switching from trigonal bipyramidal (five-coordinated Ni(II) center) to square planar (four-coordinated Ni(II) center) depending on the solvent. The equilibrium was completely shifted toward the four-coordinated Ni(II) species by addition of KPF_6 and thus trapping the halide by precipitation of KCl .³⁸

Scheme 14. Equilibria Reported in the Literature for Ni(II) Complexes with Functionalized NHC Ligands^{22e,38,39}



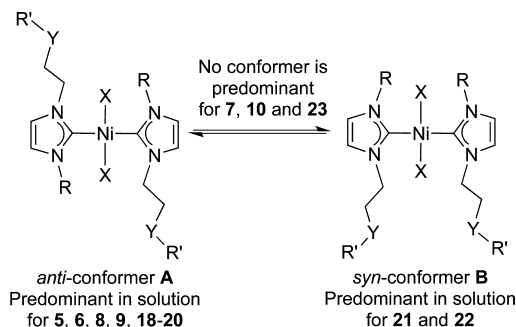
In the case of the ether/thioether-functionalized NHC complexes, no significant difference of the NMR spectrum was observed upon addition of LiBr or LiCl to the complexes. A DOSY NMR experiment revealed that the sizes of the A/B species are very similar, ruling out the formation of a dinuclear entity or the addition/removal of a ligand. Furthermore, as stated above, addition of NaBF_4 led to no reaction and thus did not affect the position of the equilibrium, which suggests that the latter does not involve halide dissociation.

Two different types of isomerization equilibria for nickel(II) complexes with functionalized NHC ligands have been reported: a *cis/trans*³⁹ or *syn/anti* isomerization (Scheme 14).^{22c,e,40} In 2007, Lee et al. described a *cis/trans* isomerization, influenced by the polarity of the solvent, of Ni(II) complexes bearing amido-functionalized NHC bidentate ligands: the *cis* isomer was highly favored in polar solvents such as $\text{DMSO}-d_6$, whereas a *cis* and *trans* mixture was obtained in the less polar CDCl_3 .³⁹ A *syn/anti* isomerization of Ni(II) complexes bearing asymmetric NHC ligands is also frequently observed^{22c,40a} and has been described in detail in the case of a monodentate amino-functionalized NHC ligand. This equilibrium does not depend on the solvent polarity.^{22e} For the *anti* species, a high-field ^1H NMR shift observed for the NCH_2 groups was induced by a spatial proximity between the amino-functionalized arm and the aromatic N-substituent of the carbene ligand. The *syn* conformation does not allow for this spatial proximity, and consequently, no shielding was observed for these NCH_2 protons. Similar shielding of an alkyl chain due to a *syn/anti* isomerization was also observed for Pd(II)-NHC complexes.⁴¹

Interestingly, the complexes **5**, **6**, **8**, **9**, **18**, **19**, **20**, **21**, and **22** present for one of their conformers similar upfield shifts for their $\text{CH}_2\text{-CH}_2\text{-Y-R}'$ protons, typical for an *anti* conformer. Furthermore, this shift was observed with $\text{R} = \text{Mes}$ or DiPP but not with $\text{R} = n\text{-Bu}$, which confirms a deshielding effect due to the aromatic character of the N-substituent of the *trans* ligand. Thus, species A is the *anti* conformer and is predominant in solution in the case of complexes $[\text{NiCl}_2(\text{NHC})_2]$ and $[\text{NiBr}_2(\text{NHC})_2]$, whereas species B, corresponding to the *syn*

conformer, is predominant in solution for the $[\text{Ni}_2(\text{NHC})_2]$ complexes (Scheme 15). Finally, the easy occurrence of *syn*/

Scheme 15. *Syn*/*Anti* Equilibrium



anti isomerization is strongly supported by the presence of positional disorder involving the presence of both conformers (*syn/anti*) in the crystal structures of **7** and **10**. In these cases, the residual electron density shown on the Fourier map did not allow for a clear discrimination between the *n*-Bu and ether arms, which display bond distances that are between C–C and C–O bonds as well as anisotropic displacement parameters that are too large for an oxygen atom and too small for a carbon atom.

Catalytic Ethylene Oligomerization. The activity of complexes **5**–**10**, **18**–**23** and **27**, **28** was assessed for the catalytic oligomerization of ethylene upon activation with

ethylaluminum dichloride (EADC) or methylaluminoxane (MAO) as cocatalyst. The influence of the cocatalyst, the *N*-substituents and additional functionality on the carbene ligands, and the nature of the halides bound to the Ni(II) center was evaluated.

The best results for **5** were obtained with EADC (vs MAO) with an improvement of the productivity from 200 to 18100 g $\text{C}_2\text{H}_4/(\text{g Ni}\cdot\text{h})$ (entries 1, 2 and 19, Table 4).

The dichlorido complexes $[\text{NiCl}_2(\text{NHC})_2]$ (**5**–**7**) displayed similar activity with *R* = Mes or DiPP, while complex **7**, with *R* = *n*-Bu, was more active (productivity: 15 000 g $\text{C}_2\text{H}_4/(\text{g Ni}\cdot\text{h})$) (entries 2–4). Similarly, among the bromido complexes $[\text{NiBr}_2(\text{NHC})_2]$ (**8**–**10**), **8** and **9** featured a similar productivity, whereas **10** was more efficient (17 500 g $\text{C}_2\text{H}_4/(\text{g Ni}\cdot\text{h})$) (entries 5–7). Unexpectedly, the trend was reversed for the diiodido complexes **21**–**23**: the best productivity was associated with the most sterically demanding NHC ligand (**21** and **22** featured higher productivity than **23**, with a smaller ligand) (entries 11–13).

For a given *R* group, the dibromido complexes **8**–**10** were more active than the dichlorido analogues **5**–**7**. No general trend was observed with the diiodido complexes.

When the size of the ether group was increased on going from an *O*-methyl group in **9** to an *O*-phenyl group in **18**, the resulting productivity drastically dropped, from 11 700 to 6100 g $\text{C}_2\text{H}_4/(\text{g Ni}\cdot\text{h})$, respectively, which highlights the importance of the size of the ether substituent (entry 8). Complex **19**, with the thioether-functionalized NHC ligand, featured an activity

Table 4. Comparative Data for Complexes **5–**10**, **18**–**23**, **27**–**29**, and $[(1\text{-H})_2(\text{NiCl}_4)]$ in Catalytic Ethylene Oligomerization^a**

entry	complex	X	R	Y-R'	ethylene consumed ^c	productivity ^d	cocatalyst ^e	selectivity ^b					
								C ₄	C ₆	C ₈ +	1-butene ^f	1-hexene ^f	linear C ₆ ^g
1	5	Cl	DiPP	OMe	0.3	200	MAO	76	18	6	82	9	24
2	5	Cl	DiPP	OMe	6.3	4600	EADC	64	32	4	52	3	17
3	6	Cl	Mes	OMe	6.1	4500	EADC	79	19	2	41	5	39
4	7	Cl	<i>n</i> -Bu	OMe	20.6	15000	EADC	75	23	2	9	1	44
5	8	Br	DiPP	OMe	17.5	12800	EADC	78	20	2	8	1	40
6	9	Br	Mes	OMe	16.0	11700	EADC	77	21	2	12	2	48
7	10	Br	<i>n</i> -Bu	OMe	24.0	17500	EADC	72	26	2	8	1	46
8	18	Br	Mes	OPh	8.4	6100	EADC	80	18	2	39	6	64
9	19	Br	DiPP	SPh	14.8	10800	EADC	78	21	1	9	1	55
10	20	Br	DiPP	CH ₂ Me	18.3	13400	EADC	80	18	2	12	2	57
11	21	I	DiPP	OMe	14.3	10400	EADC	83	15	2	12	2	45
12	22	I	Mes	OMe	18.1	13200	EADC	77	21	2	23	5	46
13	23	I	<i>n</i> -Bu	OMe	7.8	5700	EADC	86	13	1	26	7	66
14	27		Mes	OMe	22.7	16600	EADC	75	22	3	7	1	37
15	28 ^h		DiPP	CH ₂ Me	19.6	14300	EADC	62	35	3	3	1	18
16	29	Br	DiPP	DiPP	3.7	2700	EADC	38	40	22 ⁱ	76	4	12
17	$[(1\text{-H})_2(\text{NiCl}_4)]$				28.9	21100	EADC	73	24	3	6	1	39
18	ref ^j	Cl			56.2	42800	EADC	60	34	6	6	1	19
19	5	Cl	DiPP	OMe	24.8	18100	EADC ^{h,k}	77	21	2	8	1	43
20	9	Br	Mes	OMe	7.8	5700	EADC ^{h,k}	73	24	3	40	4	38
21	10	Br	<i>n</i> -Bu	OMe	21.8	15900	EADC ^{h,k}	70	27	3	9	2	47

^aConditions: amount of catalyst: 4×10^{-5} mol, *T* = 20–25 °C (except for entries 19–21, where *T* = 30 °C), solvent: toluene (except for **27** and **28**, in chlorobenzene for solubility reasons), total volume: 15 mL, 10 bar C_2H_4 , reaction time 35 min, no temperature control during reaction. Every test was repeated at least twice. ^bExpressed in wt%, calculated by GC analysis. ^cEqual to the quantity of ethylene introduced minus the unreacted ethylene collected at the end of the reaction (see Experimental Section), expressed in g. ^dExpressed in g $\text{C}_2\text{H}_4/(\text{g Ni}\cdot\text{h})$. ^eAl/Ni molar ratio: 10 (EADC) or 400 (MAO). ^fSelectivity for α -olefin within the C₄ or C₆ fraction, expressed in %. ^gSelectivity for linear olefins within the C₆ fraction. ^hThe reactor was pre-heated to 30 °C. ⁱAbout 12% octenes and 10% decenes. ^j $[\text{NiCl}_2\{\text{P}(\text{n-Bu})_3\}_2]$ tested under our conditions. ^kThe Al/Ni molar ratio was increased to 15.

similar to that of the corresponding methyl ether complex **9** (entry 9).

The effects of the temperature and of the amount of cocatalyst were also examined. Thus, the temperature was increased to 30 °C in the presence of 15 equiv of EADC instead of 10 equiv (entries 19–21). This resulted in a drastic increase of the amount of ethylene consumed for **5** (entry 19), whereas it decreased for **9** and **10** (entries 20 and 21) with a more pronounced effect for complex **9**. Thus, no linear correlation could be obtained by changing these parameters, highlighting the difficulties in rationalizing the behavior of these complexes in ethylene oligomerization.

Finally, the activity of complex **20**, with the nonfunctionalized unsymmetric NHC ligand of similar steric bulk to the ether-functionalized ligand in **8**, was assessed for comparison to evaluate the impact of the oxygen functionalization on the catalytic properties. An activity similar to that of **8** was observed, i.e., a productivity of 13 400 g C₂H₄/(g Ni·h), indicating no significant influence of the oxygen atom of the ether functionality on the catalysis (entry 10). The activity of the known symmetrical [NiBr₂{Im(DiPP)}₂] (**29**) was also assessed. A productivity of only 2700 g C₂H₄/(g Ni·h) was observed (entry 16). The improved catalytic activity of our systems compared to that of the symmetrically substituted NHC (complex **29**) may thus be related to the different steric properties of the two N-substituents. We also noted a decreased activity of the complex with the OPh substituent compared to that with the OMe moiety (entries 6 and 9).

The catalytic activity of the two cationic complexes **27** and **28** was assessed (entries 14 and 15, respectively). The catalytic activity of **27** increased compared to that of its dihalido analogue **6**, **9**, or **22**, and a productivity of 16 600 g C₂H₄/(g Ni·h) was observed. However, no improvement in the selectivity was detected. In contrast, the solution of **28** in the catalytic reactor needed to be first heated to 30 °C to lead to a productivity of 14 300 g C₂H₄/(g Ni·h), comparable to that of **20**. Both complexes required a long induction period before becoming active catalysts (see SI); the reasons are not clear but might be due to the stabilizing effect of the H-bonding interactions involving the aquo ligands.

Since we already described the active role of the [NiCl₄]²⁻ dianion in oligomerization catalysis,^{42a} the imidazolium salt [(1-H)₂(NiCl₄)] was tested for comparison and revealed a productivity of 21 100 g C₂H₄/(g Ni·h) (entry 17). Surprisingly, the productivity was higher than with the corresponding NHC complex.

The activity of the well-known phosphine nickel complex [NiCl₂{P(*n*-Bu)₃}₂] in ethylene oligomerization^{42b} was tested under the same conditions as **5**–**10**, **18**–**23**, **27**, **28**, and [(1-H)₂(NiCl₄)] and was higher than that of our NHC complexes (entry 18).

In all cases, selectivity for butene formation was observed (from 62% to 86%) with various amounts of C₆ olefins formed (from 13% to 35%) and almost no higher olefins. The formation of polyethylene was never detected. Within the butene fraction, no clear preference for 1-butene was observed. Similarly, no selectivity for 1-hexene was observed within the C₆ fraction. The selectivity for the formation of linear α -olefins increases with decreasing activity. However, variable amounts of linear olefins (from 17% to 66%) were found within the C₆ fraction, thus highlighting the isomerization tendency of nickel-based catalysts. Note that high selectivity toward linear α -

olefins could be achieved using dibromo(α -diimine)nickel complexes upon activation with MAO, MMAO, or DEAC.⁴³

CONCLUSION

High-yielding syntheses of a series of unsymmetric ether- or thioether-functionalized imidazolium salts and their corresponding bis-NHC nickel(II) halido complexes have been described in this work. All the complexes feature a *syn/anti* isomerization induced by the presence of two unsymmetric NHC ligands, and their *anti* isomers were structurally characterized. No inter- or intramolecular interaction between the ether group and the Ni(II) center was observed. Attempts to induce ether chelation by halide abstraction led to the unexpected formation of the *cis*-[Ni(NHC)₂(H₂O)₂][PF₆]₂ complexes **27** and **28**, which are rare examples of both aquo NHC complexes and of *cis* monodentate NHC ligands in Ni chemistry. All complexes were tested in catalytic ethylene oligomerization and revealed to be active with EADC as cocatalyst, with productivities up to 18 100 g C₂H₄/(g Ni·h). A comparison with nonfunctionalized unsymmetric NHC ligands revealed a similar activity, indicating a reduced role of the donor properties of the N-functionality examined (ether or thioether). In contrast, the nature of the halides bound to the Ni(II) center and the steric hindrance brought about by the N-substituent or by the R group attached to the ether or thioether of the NHC ligand significantly influenced the catalytic activity. It was generally observed that the dichlorido and the dibromido complexes with less steric hindrance on the N-substituent led to an increased activity. However, such generalization was not possible with the diiodido complexes **21**–**23**. Whether catalyst deactivation is solely due to enhanced reductive elimination, as suggested in the literature,¹⁴ cannot be stated at this stage. While the ether functionality did not lead to any remarkable activity in terms of ethylene oligomerization, this may not be the case for other nickel-based C–C coupling reactions, and this should be explored in the future. However, moderate activities were observed for the *trans* complexes, and an increase was observed with the cationic *cis* complex **27**. Further efforts on the synthesis of analogues are therefore warranted.

EXPERIMENTAL SECTION

General Considerations. All organometallic syntheses were carried out under an inert atmosphere using freshly distilled solvents and standard Schlenk techniques. Treatments for **5**, **6**, **8**, **9**, **12**, **13**, **18**–**23**, **27**, and **28** were carried out in air with nondried solvents. 1-(2,6-Diisopropylphenyl)-3-(2-methoxyethyl)-1H-imidazol-3-ium chloride ([ImH]DiPP(C₂OMe)]Cl, **1**-HCl), 1-(2,6-diisopropylphenyl)-1H-imidazol, 1-mesityl-1H-imidazole, 1-(2,6-diisopropylphenyl)-3-(*n*-butyl)-1H-imidazol-3-ium bromide ([ImH]DiPP(*n*-Bu)]Br, **17**-HBr), dibromobis[1,3-bis(2,6-diisopropylphenyl)-1,3-dihydro-2H-imidazol-2-ylidene]nickel ([NiBr₂{Im(DiPP)}₂], **27**), [NiCl₂(dme)], and [NiBr₂(dme)] were synthesized according to published procedures.^{7f,22b,30,44} All reagents were used as received from commercial suppliers. Solvents were purified and dried under argon using conventional methods.⁴⁵ ¹H NMR and ¹³C{¹H} NMR spectra were recorded on the following instruments: AVANCE I 300 MHz spectrometer, AVANCE III 400 MHz spectrometer, AVANCE I 500 MHz spectrometer, and AVANCE III 600 MHz spectrometer. The chemical shifts are given in parts per million (ppm). Data are presented as follows: chemical shift, multiplicity (s = singlet, d = doublet, t = triplet, q = quartet, m = multiplet, br = broad), coupling constant (J/Hz), and integration. Assignments were determined on the basis of either unambiguous chemical shifts, coupling patterns, or 2D correlations. The residual solvent proton (¹H) and carbon (¹³C) resonances were used as reference values. For ¹H NMR: CD₂Cl₂ =

5.32 ppm, C_6D_6 = 7.16 ppm, $(CD_3)_2CO$ = 2.05 ppm, CD_3CN = 1.95 ppm. For $^{13}C\{^1H\}$ NMR: CD_2Cl_2 = 53.8 ppm, C_6D_6 = 128.1 ppm, $(CD_3)_2CO$ = 29.8 and 206.3 ppm, CD_3CN = 1.32 and 118.3 ppm. IR spectra were recorded in the region 4000–200 cm^{-1} on a 6700 FT-IR spectrometer (ATR mode, diamond crystal). Elemental analyses were performed by the “Service de Microanalyses”, Université de Strasbourg. Mass spectrometry analyses were performed by the “Service de Spectrométrie de Masse”, Université de Strasbourg. For the X-ray diffraction studies, the intensity data were collected at 173(2) K on a Kappa CCD diffractometer 88 (graphite-monochromated Mo $K\alpha$ radiation, λ = 0.710 73 Å). Crystallographic and experimental details for all the structures are summarized in the SI. The structures were solved by direct methods (SHELXS-97) and refined by full-matrix least-squares procedures (based on F^2 , SHELXL-97) with anisotropic thermal parameters for all the non-hydrogen atoms.⁴⁶ The hydrogen atoms were introduced into the geometrically calculated positions (SHELXL-97 procedures) and refined riding on the corresponding parent atoms.

Preparation of $[(ImH)DiPP(C_2OMe)]_2[NiCl_4]$ ($[(1-H)_2(NiCl_4)]$). To a solution of the imidazolium salt $[(ImH)DiPP(C_2OMe)]Cl$ (1-HCl) (0.200 g, 0.619 mmol) in THF was added $[NiCl_2(dme)]$ (0.068 g, 0.31 mmol). The reaction mixture was stirred for 16 h. The solvent was evaporated under reduced pressure. The blue slurry was then triturated with Et_2O until a blue powder was obtained (0.198 g, 82%). MS (ESI): m/z 287.21 $[M - (NiCl_4)_{0.5}]^+$. FTIR: $\nu_{max}(solid)/cm^{-1}$ 3167w, 3093w, 3031w, 2964m, 2928w, 1565m, 1449m, 1389w, 1359m, 1311w, 1261w, 1193m, 1109s, 1095s, 1070m, 1057m, 1034w, 1013w, 969w, 958w, 936w, 876w, 860w, 834m, 811s, 765m, 750s, 738s.

Preparation of $[(ImH)Mes(C_2OMe)]Cl$ (2-HCl). A mixture of 1-mesityl-1H-imidazole (5.000 g, 26.81 mmol) and 2-chloroethyl methyl ether (25 mL, 269 mmol) was refluxed for 1.5 day. The unreacted 2-chloroethyl methyl ether was removed under reduced pressure. The resulting sticky solid was triturated twice with Et_2O . It was then stirred in THF for 16 h and collected by filtration to afford 2-HCl as a white solid. The resulting powder was dried if needed using a toluene Dean-Stark (7.470 g, 99%). 1H NMR (500 MHz, CD_2Cl_2) δ : 10.52 (t, 3J = 1.8 Hz, 1H, $CH^{imidazole}$), 8.10 (t, 3J = 1.8 Hz, 1H, $CH^{imidazole}$), 7.26 (t, 3J = 1.8 Hz, 1H, $CH^{imidazole}$), 7.01 (s, 2H, CH^{Mes}), 4.84 (t, 3J = 4.9 Hz, 2H, CH_2CH_2OMe), 3.81 (t, 3J = 4.9 Hz, 2H, CH_2CH_2OMe), 3.35 (s, 3H, CH_3^{OMe}), 2.32 (s, 3H, CH_3^{p-Mes}), 2.05 (s, 6H, CH_3^{o-Mes}). $^{13}C\{^1H\}$ NMR (126 MHz, CD_2Cl_2) δ : 141.3 (C^{Mes}), 139.0 ($CH^{imidazole}$), 134.6 (C^{Mes}), 131.2 (C^{Mes}), 129.9 (CH^{Mes}), 124.2 ($CH^{imidazole}$), 122.9 ($CH^{imidazole}$), 70.8 (CH_2CH_2OMe), 59.0 (CH_3^{OMe}), 49.9 (CH_2CH_2OMe), 21.1 (CH_3^{p-Mes}), 17.6 (CH_3^{o-Mes}). MS (ESI): m/z 245.17 $[M - Cl]^+$. FTIR: $\nu_{max}(solid)/cm^{-1}$ 3072w, 3940m, 1564m, 1542m, 1487m, 1438m, 1390m, 1294w, 1256m, 1220m, 1204m, 1189m, 1163m, 1121s, 1086m, 1066m, 1033w, 1015m, 968w, 973w, 913m, 879m, 841m, 777m, 729m, 678m, 667m, 648m.

Preparation of $[(ImH)Me(C_2OMe)]Cl$ (3-HCl). A procedure similar to that used for compound 2-HCl gave 3-HCl as a beige solid (5.345 g, 83%). 1H NMR (500 MHz, CD_2Cl_2) δ : 10.61 (s br, 1H, $CH^{imidazole}$), 7.57 (t, 3J = 1.7 Hz, 1H, $CH^{imidazole}$), 7.47 (t, 3J = 1.7 Hz, 1H, $CH^{imidazole}$), 4.55 (t, 3J = 4.8 Hz, 2H, CH_2CH_2OMe), 4.03 (s, 3H, CH_3), 3.74 (t, 3J = 4.8 Hz, 2H, CH_2CH_2OMe), 3.33 (s, 3H, CH_3^{OMe}). $^{13}C\{^1H\}$ NMR (126 MHz, CD_2Cl_2) δ : 138.6 ($CH^{imidazole}$), 123.2 ($CH^{imidazole}$), 123.1 ($CH^{imidazole}$), 70.7 (CH_2CH_2OMe), 59.1 (CH_3^{OMe}), 49.9 (CH_2CH_2OMe), 36.6 (CH_3). MS (ESI): m/z 141.10 $[M - Cl]^+$. FTIR: $\nu_{max}(solid)/cm^{-1}$ 3073w, 2935m, 1562m, 1444m, 1369m, 1336m, 1289w, 1262m, 1224w, 1191m, 1168m, 1113s, 1076s, 1010m, 959w, 909m, 847m, 802s, 699m, 660s, 631m.

Preparation of $[(ImH)n-Bu(C_2OMe)]Cl$ (4-HCl). A procedure similar to that used for compound 2-HCl gave 4-HCl as a colorless oil (9.563 g, 82%). 1H NMR (500 MHz, CD_2Cl_2) δ : 10.57 (t, 3J = 1.8 Hz, 1H, $CH^{imidazole}$), 7.69 (t, 3J = 1.8 Hz, 1H, $CH^{imidazole}$), 7.60 (t, 3J = 1.8 Hz, 1H, $CH^{imidazole}$), 4.53 (t, 3J = 4.7 Hz, 2H, CH_2CH_2OMe), 4.25 (t, 3J = 7.3 Hz, 2H, $CH_2CH_2CH_2CH_3^{nBu}$), 3.69 (t, 3J = 4.7 Hz, 2H, CH_2CH_2OMe), 3.26 (s, 3H, CH_3^{OMe}), 1.91–1.70 (m, 2H, $CH_2CH_2CH_2CH_3^{nBu}$), 1.34–1.21 (m, 2H, $CH_2CH_2CH_2CH_3^{nBu}$), 0.86 (t, 3J = 7.4 Hz, 3H, $CH_2CH_2CH_2CH_3^{nBu}$). $^{13}C\{^1H\}$ NMR (126

MHz, CD_2Cl_2) δ : 137.7 ($CH^{imidazole}$), 123.1 ($CH^{imidazole}$), 121.9 ($CH^{imidazole}$), 70.5 (CH_2CH_2OMe), 58.8 (CH_3^{OMe}), 49.6 ($CH_2CH_2CH_2CH_3^{nBu}$), 49.5 (CH_2CH_2OMe), 32.1 ($CH_2CH_2CH_2CH_3^{nBu}$), 19.5 ($CH_2CH_2CH_2CH_3^{nBu}$), 13.3 (CH_3^{nBu}). MS (ESI): m/z 183.15 $[M - Cl]^+$. FTIR: $\nu_{max}(solid)/cm^{-1}$: 2933w, 1562m, 1460m, 1357w, 1264m, 1167s, 1115s, 1081m, 1014m, 969w, 879w, 833m, 754m, 648m.

Preparation of $[NiCl_2(ImDiPP(C_2OMe))]_2$ (5). To a solution of the imidazolium salt 1-HCl (0.520 g, 1.61 mmol) in toluene (10 mL) was added KHMDS (0.418 g, 2.09 mmol). The reaction mixture was stirred for 1 h, and the brown precipitate was eliminated by filtration from the colorless solution. To this solution was added $[NiCl_2(dme)]$ (0.177 g, 0.806 mmol). The reaction mixture was stirred for 3 h. The orange solution was then filtered through a Celite pad, the Celite was washed several times with toluene, and the filtrate was evaporated under reduced pressure. The complex was precipitated from THF/pentane and washed with pentane to afford an orange powder of 5. If needed, this powder can be washed with H_2O and solubilized in toluene, the solution dried with Na_2SO_4 , and the solvent removed under reduced pressure (0.440 g, 77%). *Anti*-form: 1H NMR (C_6D_6 , 500 MHz) δ : 7.37 (t, 3J = 7.1 Hz, 2H, CH^{p-Ar}), 7.32 (d, 3J = 7.1 Hz, 4H, CH^{m-Ar}), 6.66 (d, 3J = 1.7 Hz, 2H, $CH^{imidazole}$), 6.33 (d, 3J = 1.7 Hz, 2H, $CH^{imidazole}$), 4.96 (t, 3J = 4.8 Hz, 4H, CH_2CH_2OMe), 3.85 (t, 3J = 4.3 Hz, 4H, CH_2CH_2OMe), 3.13 (sept, 3J = 6.7 Hz, 4H, CH^{iPr}), 3.01 (s, 6H, CH_3^{OMe}), 1.53 (d, 3J = 6.6 Hz, 12H, CH_3^{iPr}), 0.92 (d, 3J = 6.9 Hz, 12H, CH_3^{iPr}). $^{13}C\{^1H\}$ NMR (126 MHz, C_6D_6) δ : 171.5 ($C^{carbene}$), 148.4 (C^{Ar}), 136.7 (C^{Ar}), 129.9 (CH^{Ar}), 123.9 (CH^{Ar}), 123.6 ($CH^{imidazole}$), 121.7 ($CH^{imidazole}$), 72.3 (CH_2CH_2OMe), 58.7 (CH_3^{OMe}), 51.5 (CH_2CH_2OMe), 28.7 (CH^{iPr}), 26.8 (CH_3^{iPr}), 23.0 (CH_3^{iPr}). *Syn*-form: 1H NMR (500 MHz, C_6D_6) δ : 7.38 (t, 3J = 7.8 Hz, 2H, CH^{p-Ar}), 7.19 (d, 3J = 7.8 Hz, 4H, CH^{m-Ar}), 6.66 (d, 3J = 1.6 Hz, 2H, $CH^{imidazole}$), 6.26 (d, 3J = 1.6 Hz, 2H, $CH^{imidazole}$), 5.65 (t, 3J = 5.3 Hz, 4H, CH_2CH_2OMe), 4.18 (t, 3J = 5.4 Hz, 4H, CH_2CH_2OMe), 3.08 (s, 6H, CH_3^{OMe}), 2.91 (sept, 3J = 6.7 Hz, 4H, CH^{iPr}), 1.21 (d, 3J = 6.7 Hz, 12H, CH_3^{iPr}), 0.91 (d, 3J = 6.7 Hz, 12H, CH_3^{iPr}). $^{13}C\{^1H\}$ NMR (C_6D_6 , 126 MHz) δ : 170.2 ($C^{carbene}$), 147.3 (C^{Ar}), 136.3 (C^{Ar}), 129.7 (CH^{Ar}), 124.1 (CH^{Ar}), 124.0 ($CH^{imidazole}$), 121.4 ($CH^{imidazole}$), 72.8 (CH_2CH_2OMe), 58.8 (CH_3^{OMe}), 51.4 (CH_2CH_2OMe), 28.4 (CH^{iPr}), 26.5 (CH_3^{iPr}), 23.3 (CH_3^{iPr}). MS (ESI): m/z 665.31 $[M - Cl]^+$. FTIR: $\nu_{max}(solid)/cm^{-1}$ 3133vw, 2964m, 2865m, 1466m, 1446m, 1413m, 1380m, 1356m, 1321w, 1292m, 1269m, 1181m, 1162vw, 1120s, 1089vw, 1059w, 1040w, 1011m, 957m, 933w, 897vw, 843w, 822w, 803m, 762s, 735m, 706s, 641w, 614w, 567m, 536s, 474m, 427m, 392vs, 350m, 316w, 275w, 225m, 128vs. Anal. Calcd for $C_{36}H_{52}Cl_2N_4NiO_2$: C, 61.56; H, 7.64; N, 7.98. Found: C, 61.57; H, 7.46; N, 7.94.

Preparation of $[NiCl_2(ImMes(C_2OMe))]_2$ (6). A procedure similar to that used for compound 5 gave 6 as an orange solid (0.446 g, 81%). *Anti*-form: 1H NMR (C_6D_6 , 500 MHz) δ : 6.94 (s, 4H, CH^{Mes}), 6.52 (d, 3J = 1.7 Hz, 2H, $CH^{imidazole}$), 5.89 (d, 3J = 1.7 Hz, 2H, $CH^{imidazole}$), 4.90 (t, 3J = 4.8 Hz, 4H, CH_2CH_2OMe), 4.07 (t, 3J = 4.8 Hz, 4H, CH_2CH_2OMe), 3.09 (s, 6H, CH_3^{OMe}), 2.38 (s, 12H, CH_3^{o-Mes}), 2.25 (s, 6H, CH_3^{p-Mes}). $^{13}C\{^1H\}$ NMR (126 MHz, C_6D_6) δ : 169.8 ($C^{carbene}$), 137.6 (C^{Mes}), 137.1 (C^{Mes}), 136.8 (C^{Mes}), 129.1 (CH^{Mes}), 122.5 ($CH^{imidazole}$), 121.4 ($CH^{imidazole}$), 72.7 (CH_2CH_2OMe), 58.7 (CH_3^{OMe}), 51.3 (CH_2CH_2OMe), 21.2 (CH_3^{p-Mes}), 19.6 (CH_3^{o-Mes}). *Syn*-form: 1H NMR (C_6D_6 , 500 MHz) δ : 6.89 (s, 4H, CH^{Mes}), 6.55 (d, 3J = 1.8 Hz, 2H, $CH^{imidazole}$), 5.86 (d, 3J = 1.8 Hz, 2H, $CH^{imidazole}$), 5.35 (t, 3J = 5.3 Hz, 4H, CH_2CH_2OMe), 4.26 (t, 3J = 5.3 Hz, 4H, CH_2CH_2OMe), 3.12 (s, 6H, CH_3^{OMe}), 2.40 (s, 6H, CH_3^{p-Mes}), 2.16 (s, 12H, CH_3^{o-Mes}). $^{13}C\{^1H\}$ NMR (126 MHz, C_6D_6) δ : 170.2 ($C^{carbene}$), 138.2 (C^{Mes}), 137.3 (C^{Mes}), 136.7 (C^{Mes}), 129.4 (CH^{Mes}), 122.1 ($CH^{imidazole}$), 121.9 ($CH^{imidazole}$), 72.9 (CH_2CH_2OMe), 58.8 (CH_3^{OMe}), 51.2 (CH_2CH_2OMe), 21.5 (CH_3^{p-Mes}), 19.2 (CH_3^{o-Mes}). MS (ESI): m/z 581.22 $[M - Cl]^+$. FTIR: $\nu_{max}(solid)/cm^{-1}$ 3173w, 3141w, 2919m, 1852m, 2831m, 1489m, 1447m, 1412m, 1395m, 1379w, 1355m, 1300w, 1259m, 1216m, 1183m, 1166w, 119s, 1094m, 1080m, 1035m, 1001m, 961vw, 935m, 901w, 858m, 840m, 827w, 734m, 706s, 641m, 588m, 575w, 562w, 537w, 467w, 406m, 359m,

195m. Anal. Calcd for $C_{30}H_{40}Cl_2N_4NiO_2$: C, 58.28; H, 6.52; N, 9.06. Found: C, 58.24; H, 6.53; N, 8.86.

Preparation of $[NiCl_2\{Imn-Bu(C_2O_2Me)\}_2]$ (7). To a solution of the silver complex **13** (0.500 g, 0.985 mmol) in THF (15 mL) was added solid $[NiCl_2(dme)]$ (0.216 g, 0.983 mmol). The reaction mixture turned orange, a white precipitate of AgCl formed, and stirring was maintained overnight. Then, THF was removed under reduced pressure, the orange residue was redissolved in toluene, and the white suspension of AgCl was filtered off through Celite. The orange filtrate was precipitated with pentane, and the orange powder washed several times with pentane to afford the desired complex **7** (0.316 g, 65%). Most signals of both conformers (*syn*- and *anti*-form) overlapped. 1H NMR (500 MHz, C_6D_6) δ : 6.52 (s br, 2H, $CH^{imidazole}$), 6.06 (s br, 2H, $CH^{imidazole}$), 5.32–5.15 (m br, 4H, $CH_2CH_2O_2Me$), 4.94–4.79 (m br, 4H, $CH_2CH_2CH_2CH_3^{nBu}$), 4.26–4.15 (m br, 4H, $CH_2CH_2O_2Me$), 3.11 (s, 3H, CH_3^{OMe}), 3.09 (s, 3H, CH_3^{OMe}), 2.32–2.18 (m br, 4H, $CH_2CH_2CH_2CH_3^{nBu}$), 1.55–1.40 (m br, 4H, $CH_2CH_2CH_2CH_3^{nBu}$), 1.08–0.93 (m br, 6H, $CH_2CH_2CH_2CH_3^{nBu}$). $^{13}C\{^1H\}$ NMR (126 MHz, C_6D_6) δ : 169.8 ($C^{carbene}$), 121.8 ($CH^{imidazole}$), 121.8 ($CH^{imidazole}$), 119.8 ($CH^{imidazole}$), 119.9 ($CH^{imidazole}$), 72.8 ($CH_2CH_2O_2Me$), 72.8 ($CH_2CH_2O_2Me$), 58.8 (CH_3^{OMe}), 58.8 (CH_3^{OMe}), 50.9 ($CH_2CH_2O_2Me$), 50.6 ($CH_2CH_2CH_2CH_3^{nBu}$), 50.6 ($CH_2CH_2CH_2CH_3^{nBu}$), 33.5 ($CH_2CH_2CH_2CH_3^{nBu}$), 33.5 ($CH_2CH_2CH_2CH_3^{nBu}$), 20.6 ($CH_2CH_2CH_2CH_3^{nBu}$), 20.6 ($CH_2CH_2CH_2CH_3^{nBu}$), 14.1 (CH_3^{nBu}), 14.1 (CH_3^{nBu}). MS (ESI): m/z 457.19 $[M - Cl]^+$. FTIR: $\nu_{max}(solid)/cm^{-1}$ 3125m, 2932m, 2874m, 1457m, 1422m, 1358m, 1342m, 1266m, 1241m, 1225m, 1197m, 1119s, 1087m, 1038m, 1010m, 966m, 8807w, 804w, 754m, 706s, 668w, 535m, 520m, 458m, 391s. Anal. Calcd for $C_{20}H_{36}Cl_2N_4NiO_2$: C, 48.61; H, 7.34; N, 11.34. Found: C, 47.95; H, 7.40; N, 10.57. Despite several attempts, better results could not be obtained.

Preparation of $[NiBr_2\{ImDiPP(C_2O_2Me)\}_2]$ (8). To a solution of imidazolium salt **1**·HCl (0.677 g, 2.10 mmol) in toluene (10 mL) was added KHMDS (0.544 g, 2.73 mmol). The reaction mixture was stirred for 1 h, and the brown precipitate was eliminated by filtration from the colorless solution. To this solution was added $[NiBr_2(dme)]$ (0.324 g, 1.05 mmol). The reaction mixture turned instantaneously red and was stirred for 3 h. It was then filtered through a Celite pad, which was washed several times with toluene, and the filtrate was evaporated under reduced pressure. The complex was washed with cold pentane to afford a red powder of **8**. If needed, the resulting powder could be washed with H_2O and solubilized in toluene, and the solution dried with Na_2SO_4 . The solvent was removed under reduced pressure (0.669 g, 81%). *Anti*-form: 1H NMR (C_6D_6 , 500 MHz) δ : 7.38–7.33 (m, 2H, CH^{p-Ar}), 7.30 (d, $^3J = 7.1$ Hz, 4H, CH^{m-Ar}), 6.70 (d, $^3J = 1.5$ Hz, 2H, $CH^{imidazole}$), 6.35 (d, $^3J = 1.5$ Hz, 2H, $CH^{imidazole}$), 5.02 (t, $^3J = 4.9$ Hz, 4H, $CH_2CH_2O_2Me$), 3.83 (t, $^3J = 4.9$ Hz, 4H, $CH_2CH_2O_2Me$), 3.27 (sept, $^3J = 6.6$ Hz, 4H, CH^{iPr}), 3.00 (s, 6H, CH_3^{OMe}), 1.56 (d, $^3J = 6.6$ Hz, 12H, CH_3^{iPr}), 0.91 (d, $^3J = 6.9$ Hz, 12H, CH_3^{iPr}). $^{13}C\{^1H\}$ NMR (C_6D_6 , 126 MHz) δ : 172.6 ($C^{carbene}$), 148.3 (C^{Ar}), 136.4 (C^{Ar}), 130.1 (CH^{Ar}), 124.5 ($CH^{imidazole}$), 123.9 (CH^{Ar}), 122.0 ($CH^{imidazole}$), 71.8 ($CH_2CH_2O_2Me$), 58.6 (CH_3^{OMe}), 51.8 ($CH_2CH_2O_2Me$), 28.9 (CH^{iPr}), 26.9 (CH_3^{iPr}), 23.3 (CH_3^{iPr}). *Syn*-form: 1H NMR (C_6D_6 , 500 MHz) δ : 7.39–7.32 (m, 2H, CH^{p-Ar}), 7.17 (d, $^3J = 7.1$ Hz, 4H, CH^{m-Ar}), 6.70 (d, $^3J = 1.5$ Hz, 2H, $CH^{imidazole}$), 6.29 (d, $^3J = 1.5$ Hz, 2H, $CH^{imidazole}$), 5.67 (t, $^3J = 5.3$ Hz, 4H, $CH_2CH_2O_2Me$), 4.19 (t, $^3J = 5.3$ Hz, 4H, $CH_2CH_2O_2Me$), 3.09 (s, 2H, CH_3^{OMe}), 3.06–3.01 (m, 4H, CH^{iPr}), 1.23 (d, $^3J = 6.6$ Hz, 12H, CH_3^{iPr}), 0.90 (d, $^3J = 6.6$ Hz, 12H, CH_3^{iPr}). $^{13}C\{^1H\}$ NMR (126 MHz, C_6D_6) δ : 171.7 ($C^{carbene}$), 147.2 (C^{Ar}), 136.1 (C^{Ar}), 129.8 (CH^{Ar}), 124.8 ($CH^{imidazole}$), 124.3 (CH^{Ar}), 121.8 ($CH^{imidazole}$), 72.2 ($CH_2CH_2O_2Me$), 58.8 (CH_3^{OMe}), 51.8 ($CH_2CH_2O_2Me$), 28.5 (CH^{iPr}), 26.7 (CH_3^{iPr}), 23.4 (CH_3^{iPr}). MS (ESI): m/z 711.25 $[M - Br]^+$. FTIR: $\nu_{max}(solid)/cm^{-1}$ 3135w, 2963m, 2933m, 2865m, 1460m, 1445m, 1411m, 1380m, 1358m, 1319w, 1290m, 1269m, 1209m, 1181m, 1119m, 1078m, 1057m, 1041m, 1010m, 956m, 933w, 896vw, 842w, 821w, 802m, 759s, 733m, 704s, 640m, 613w, 566m, 531w, 474m, 425w, 355m, 219m. Anal. Calcd for $C_{36}H_{52}Br_2N_4NiO_2$: C, 54.64; H, 6.62; N, 7.08. Found: C, 54.66; H, 6.37; N 7.00.

Preparation of $[NiBr_2\{ImMes(C_2O_2Me)\}_2]$ (9). A procedure similar to that used for compound **8** gave **9** as a red solid (0.547 g, 87%). *Anti*-form: 1H NMR (500 MHz, C_6D_6) δ : 6.92 (s, 4H, CH^{Mes}), 6.56 (d, $^3J = 1.8$ Hz, 2H, $CH^{imidazole}$), 5.89 (d, $^3J = 1.8$ Hz, 2H, $CH^{imidazole}$), 4.96 (t, $^3J = 5.0$ Hz, 4H, $CH_2CH_2O_2Me$), 4.03 (t, $^3J = 5.0$ Hz, 4H, $CH_2CH_2O_2Me$), 3.10 (s, 6H, CH_3^{OMe}), 2.42 (s, 12H, CH_3^{o-Mes}), 2.23 (s, 6H, CH_3^{o-Mes}). $^{13}C\{^1H\}$ NMR (126 MHz, C_6D_6) δ : 171.1 ($C^{carbene}$), 138.2 (C^{Mes}), 137.5 (C^{Mes}), 136.9 (C^{Mes}), 129.2 (CH^{Mes}), 122.8 ($CH^{imidazole}$), 122.4 ($CH^{imidazole}$), 72.1 ($CH_2CH_2O_2Me$), 58.7 (CH_3^{OMe}), 51.6 ($CH_2CH_2O_2Me$), 21.1 (CH_3^{p-Mes}), 20.5 (CH_3^{o-Mes}). *Syn*-form: 1H NMR (500 MHz, C_6D_6) δ : 6.85 (s, 4H, CH^{Mes}), 6.61 (d, $^3J = 1.8$ Hz, 2H, $CH^{imidazole}$), 5.86 (d, $^3J = 1.8$ Hz, 2H, $CH^{imidazole}$), 5.41 (t, $^3J = 5.3$ Hz, 4H, $CH_2CH_2O_2Me$), 4.19 (t, $^3J = 5.3$ Hz, 4H, $CH_2CH_2O_2Me$), 3.12 (s, 6H, CH_3^{OMe}), 2.39 (s, 6H, CH_3^{p-Mes}), 2.19 (s, 12H, CH_3^{o-Mes}). $^{13}C\{^1H\}$ NMR (126 MHz, C_6D_6) δ : 171.3 ($C^{carbene}$), 137.4 (C^{Mes}), 136.7 (C^{Mes}), 136.4 (C^{Mes}), 129.5 (CH^{Mes}), 122.9 ($CH^{imidazole}$), 122.4 ($CH^{imidazole}$), 72.2 ($CH_2CH_2O_2Me$), 58.7 (CH_3^{OMe}), 51.6 ($CH_2CH_2O_2Me$), 21.4 (CH_3^{p-Mes}), 20.0 (CH_3^{o-Mes}). MS (ESI): m/z 625.16 $[M - Br]^+$. FTIR: $\nu_{max}(solid)/cm^{-1}$ 3173w, 3143w, 2919m, 1850m, 1830m, 1486m, 1448m, 1411m, 1392m, 1355m, 1298w, 1257m, 1216m, 1182m, 1166w, 1119s, 1093m, 1079m, 1034m, 1000m, 933m, 857m, 839m, 824m, 739m, 704s, 694s, 640m, 588s, 874w, 536m, 467w, 39m, 326m, 309s, 197s. Anal. Calcd for $C_{30}H_{40}Br_2N_4NiO_2$: C, 50.95; H, 5.70; N, 7.92. Found: C, 51.00; H, 5.79; N, 7.95.

Preparation of $[NiBr_2\{Imn-Bu(C_2O_2Me)\}_2]$ (10). Method A: A procedure similar to that used for compound **8** gave **10** as a red solid (0.190 g, 33%). Method B: The nickel complex **7** (0.055 g, 0.11 mmol) was dissolved in acetone, and solid LiBr (0.029 g, 0.33 mmol) was added. The orange solution immediately turned pink and was stirred overnight. The solvent was evaporated under reduced pressure, and the product redissolved in toluene. A white precipitate of LiCl (insoluble in toluene) was filtered off through Celite, and the solvent was removed under reduced pressure. The complex was washed with pentane to afford a red powder of **10** (0.052 g, 81%). Most signals of both conformers (*syn*- and *anti*-forms) overlapped. 1H NMR (300 MHz, C_6D_6) δ : 6.61–6.44 (m, 2H, $CH^{imidazole}$), 6.14 (s br, 2H, $CH^{imidazole}$), 5.27–5.00 (m, 4H, $CH_2CH_2O_2Me$), 4.91–4.75 (m, 4H, $CH_2CH_2CH_2CH_3^{nBu}$), 4.24–4.07 (m, 4H, $CH_2CH_2O_2Me$), 3.12 (s, 3H, CH_3^{OMe}), 3.10 (s, 3H, CH_3^{OMe}), 2.28–2.06 (m, 4H, $CH_2CH_2CH_2CH_3^{nBu}$), 1.53–1.36 (m, 4H, $CH_2CH_2CH_2CH_3^{nBu}$), 1.04–0.88 (m, 6H, $CH_2CH_2CH_2CH_3^{nBu}$). $^{13}C\{^1H\}$ NMR (126 MHz, C_6D_6) δ : 171.4 ($C^{carbene}$), 171.3 ($C^{carbene}$), 122.4 ($CH^{imidazole}$), 122.4 ($CH^{imidazole}$), 120.5 ($CH^{imidazole}$), 120.5 ($CH^{imidazole}$), 72.2 ($CH_2CH_2O_2Me$), 72.2 ($CH_2CH_2O_2Me$), 58.8 (CH_3^{OMe}), 58.7 (CH_3^{OMe}), 51.0 ($CH_2CH_2O_2Me$), 51.0 ($CH_2CH_2O_2Me$), 50.8 ($CH_2CH_2CH_2CH_3^{nBu}$), 50.8 ($CH_2CH_2CH_2CH_3^{nBu}$), 32.9 ($CH_2CH_2CH_2CH_3^{nBu}$), 32.9 ($CH_2CH_2CH_2CH_3^{nBu}$), 20.6 ($CH_2CH_2CH_2CH_3^{nBu}$), 20.6 ($CH_2CH_2CH_2CH_3^{nBu}$), 14.1 (CH_3^{nBu}), 14.1 (CH_3^{nBu}). MS (ESI): m/z 503.13 $[M - Br]^+$. FTIR: $\nu_{max}(solid)/cm^{-1}$ 3133w, 2961m, 2933m, 2873m, 1457m, 1420m, 1376w, 1357m, 1265m, 1224m, 1198m, 1176m, 1112s, 1036m, 1008m, 831m, 730m, 695s, 668m, 567w, 535w, 378m, 316m. Anal. Calcd for $C_{20}H_{36}Br_2N_4NiO_2$: C, 41.20; H, 6.22; N, 9.61. Found: C, 41.29; H, 6.55; N, 8.72. Despite several attempts, better analytical results could not be obtained.

Isolation of $[(ImH)DiPP(C_2O_2Me)][NiCl_3\{ImDiPP(C_2O_2Me)\}_2]$ (11). In the workup of the reaction that produced **5**, crystallization was performed by slow evaporation from the crude reaction mixture solubilized in toluene. A few blue crystals of **11** were isolated even though **5** was the major product.

Preparation of $[Ag\{ImMe(C_2O_2Me)\}_2]Cl$ (12). A mixture of the imidazolium salt **3**·HCl (1.362 g, 7.711 mmol), Ag_2O (0.983 g, 4.24 mmol), and molecular sieves in MeOH (30 mL) was stirred under exclusion of light for 16 h. The beige reaction mixture was then filtered through Celite, and the filtrate dried under reduced pressure. The resulting solid was dissolved in the minimum amount of CH_2Cl_2 and precipitated by addition of Et_2O to afford **12** as a beige powder (1.427 g, 87%). 1H NMR (300 MHz, CD_2Cl_2) δ : 7.22 (d, $^3J = 1.7$ Hz, 2H, $CH^{imidazole}$), 7.10 (d, $^3J = 1.7$ Hz, 2H, $CH^{imidazole}$), 4.40 (t, $^3J = 4.9$ Hz,

4H, CH₂CH₂OMe), 3.89 (s, 6H, CH₃), 3.70 (t, ³J = 4.9 Hz, 4H, CH₂CH₂OMe), 3.31 (s, 6H, CH₃^{OMe}). ¹³C{¹H} NMR (126 MHz, CD₂Cl₂) δ: 183.3 (C^{carbene}), 122.4 (CH^{imidazole}), 122.3 (CH^{imidazole}), 72.6 (CH₂CH₂OMe), 59.1 (CH₃^{OMe}), 52.0 (CH₂CH₂OMe), 38.9 (CH₃). MS (ESI): *m/z* 387.09 [M – Cl]⁺. FTIR: $\nu_{\text{max}}(\text{solid})/\text{cm}^{-1}$ 3073w, 2071w, 1670m, 1653m, 1566w, 1458m, 1410m, 1358m, 1273m, 1244m, 1210m, 1187m, 1109s, 1079s, 1045w, 1032w, 1009m, 962w, 864w, 846m, 757s, 732s, 669m, 531m, 459m, 337m, 256m, 230m. Anal. Calcd for C₁₄H₂₄AgClN₄O₂: C, 39.69; H, 5.71; N, 13.22. Found: C, 37.10; H, 6.07; N, 12.69. Despite several attempts, better analytical results could not be obtained.

Preparation of [Ag{Imn-Bu(C₂OMe)}₂]Cl (13). A procedure similar to that used for compound 12 gave **13** as a white solid (1.105 g, 75%). ¹H NMR (300 MHz, CD₂Cl₂) δ: 7.25 (d, ³J = 1.7 Hz, 2H, CH^{imidazole}), 7.09 (d, ³J = 1.7 Hz, 2H, CH^{imidazole}), 4.41 (t, ³J = 5.0 Hz, 4H, CH₂CH₂OMe), 4.16 (t, ³J = 7.2 Hz, 4H, CH₂CH₂CH₂CH₃^{nBu}), 3.72 (t, ³J = 5.0 Hz, 4H, CH₂CH₂OMe), 3.32 (s, 6H, CH₃^{OMe}), 1.88–1.78 (m, 4H, CH₂CH₂CH₂CH₃^{nBu}), 1.42–1.30 (m, 4H, CH₂CH₂CH₂CH₃^{nBu}), 0.95 (t, ³J = 7.3 Hz, 6H, CH₂CH₂CH₂CH₃^{nBu}). ¹³C{¹H} NMR (75 MHz, CD₂Cl₂) δ: 180.8 (C^{carbene}), 122.3 (CH^{imidazole}), 121.3 (CH^{imidazole}), 72.2 (CH₂CH₂OMe), 58.9 (CH₃^{OMe}), 51.9 (CH₂CH₂OMe), 51.8 (CH₂CH₂CH₂CH₃^{nBu}), 33.7 (CH₂CH₂CH₂CH₃^{nBu}), 19.9 (CH₂CH₂CH₂CH₃^{nBu}), 13.6 (CH₃^{nBu}). MS (ESI): *m/z* 473.19 [M – Cl]⁺. FTIR: $\nu_{\text{max}}(\text{solid})/\text{cm}^{-1}$ 3055m, 2930m, 1456m, 1419m, 1363m, 1342m, 1248m, 1224m, 1201m, 1113s, 1079m, 1047m, 1007m, 970w, 834m, 789m, 755m, 685w, 675m, 530w, 560m, 325w, 219m. Anal. Calcd for C₂₀H₃₆AgClN₄O₂: C, 47.30; H, 7.15; N, 11.03. Found: C, 44.96; H, 7.33; N, 10.58. Despite several attempts, better analytical results could not be obtained.

Preparation of [(ImH)Mes(C₂OPh)]Cl (15-HCl). A procedure similar to that used for compound 2-HCl gave **15-HCl** as a beige solid (2.202 g, 83%). ¹H NMR (500 MHz, CD₂Cl₂) δ: 10.68 (s br, 1H, CH^{imidazole}), 8.08 (s br, 1H, CH^{imidazole}), 7.31–7.25 (m, 2H, CH^{o-Ph}), 7.20 (t, ³J = 1.8 Hz, 1H, CH^{imidazole}), 7.03 (s, 2H, CH^{Mes}), 7.00–6.96 (m, 1H, CH^{p-Ph}), 6.95–6.89 (m, 2H, CH^{m-Ph}), 5.17 (t, ³J = 4.8 Hz, 2H, CH₂CH₂OPh), 4.49 (t, ³J = 4.8 Hz, 2H, CH₂CH₂OPh), 2.34 (s, 3H, CH₃^{p-Mes}), 2.05 (s, 6H, CH₃^{o-Mes}). ¹³C{¹H} NMR (126 MHz, CD₂Cl₂) δ: 158.1 (C^{OPh}), 141.6 (C^{Mes}), 139.3 (CH^{imidazole}), 134.7 (C^{Mes}), 131.2 (C^{Mes}), 130.0 (CH^{OPh}), 129.9 (CH^{Mes}), 124.3 (CH^{imidazole}), 123.1 (CH^{imidazole}), 121.9 (CH^{OPh}), 114.8 (CH^{OPh}), 66.9 (CH₂CH₂OPh), 49.9 (CH₂CH₂OPh), 21.2 (CH₃^{p-Mes}), 17.7 (CH₃^{o-Mes}). MS (ESI): *m/z* 307.18 [M – Cl]⁺. FTIR: $\nu_{\text{max}}(\text{solid})/\text{cm}^{-1}$ 2969m, 1589m, 1560m, 1548m, 1489m, 1461m, 1418w, 1396w, 1369w, 1332w, 1307w, 1293m, 1236m, 1208m, 1171m, 1107w, 1081m, 1070m, 1050m, 983w, 939w, 909m, 898m, 877m, 791m, 754s, 731m, 692s, 674m, 665m, 641m, 612w.

Preparation of [(ImH)DiPP(C₂SPh)]Cl (16-HCl). The reagents 1-(2,6-diisopropylphenyl)-1H-imidazol (1.55 g, 6.79 mmol) and 2-chloroethyl phenyl sulfide (2.00 mL, 2.34 g, 13.6 mmol) were charged in an Ace pressure tube and heated at 120 °C for 2 h. The resulting brown residue was precipitated several times from a MeOH/Et₂O mixture, affording the imidazolium salt **16-HCl** as an off-gray powder. The latter was dried if needed using a toluene Dean–Stark (1.960 g, 72%). ¹H NMR (500 MHz, CD₂Cl₂) δ: 10.44 (s br, 1H, CH^{imidazole}), 8.16 (s br, 1H, CH^{imidazole}), 7.56 (t, ³J = 7.8 Hz, 1H, CH^{p-DiPP}), 7.45–7.37 (m, 2H, CH^{p-SPh}), 7.37–7.32 (m, 4H, CH^{m-DiPP} + CH^{m-SPh}), 7.29–7.22 (m, 1H, CH^{p-SPh}), 7.18 (s br, 1H, CH^{imidazole}), 4.92 (t, ³J = 5.9 Hz, 2H, CH₂CH₂SPh), 3.70 (t, ³J = 5.9 Hz, 2H, CH₂CH₂SPh), 2.31 (septet, ³J = 6.8 Hz, 2H, CH^{iPr}), 1.20 (d, ³J = 6.8 Hz, 6H, CH₃^{iPr}), 1.15 (d, ³J = 6.8 Hz, 6H, CH₃^{iPr}). ¹³C{¹H} NMR (126 MHz, CD₂Cl₂) δ: 145.8 (C^{DiPP}), 139.3 (CH^{imidazole}), 134.1 (C^{SPh}), 132.2 (CH^{DiPP}), 130.6 (C^{DiPP}), 130.1 (CH^{SPh}), 129.8 (CH^{SPh}), 127.4 (CH^{SPh}), 124.9 (CH^{DiPP}), 124.4 (CH^{imidazole}), 124.1 (CH^{imidazole}), 49.2 (CH₂CH₂SPh), 35.1 (CH₂CH₂SPh), 29.0 (CH^{iPr}), 24.5 (CH₃^{iPr}), 24.2 (CH₃^{iPr}). MS (ESI): *m/z* 365.20 [M – Cl]⁺. FTIR: $\nu_{\text{max}}(\text{solid})/\text{cm}^{-1}$ 2961m, 1559m, 1541m, 1458m, 1438m, 1386w, 1365m, 1313w, 1264w, 1191m, 1109m, 1089m, 1070m, 1059m, 1024m, 957w, 937w, 804m, 739s, 691m, 671m, 639m, 614w.

Preparation of [NiBr₂{ImMes(C₂OPh)}₂] (18). A procedure similar to that used for compound **8** gave **18** as a red solid (0.470

g, 81%). *Anti*-form: ¹H NMR (300 MHz, C₆D₆) δ: 7.14–7.03 (m, 2H, CH^{OPh}), 6.98–6.77 (m, 8H, CH^{OPh}), 6.88 (s, 4H, CH^{Mes}), 6.55–6.44 (m, 2H, CH^{imidazole}), 5.88 (d, ³J = 1.7 Hz, 2H, CH^{imidazole}), 5.11 (t, ³J = 5.0 Hz, 4H, CH₂CH₂OPh), 4.59 (t, ³J = 5.0 Hz, 4H, CH₂CH₂OPh), 2.37 (s, 6H, CH₃^{p-Mes}), 2.17 (s, 12H, CH₃^{p-Mes}). ¹³C{¹H} NMR (101 MHz, C₆D₆) δ: 171.6 (C^{carbene}), 159.2 (C^{OPh}), 138.5 (C^{Mes}), 137.4 (C^{Mes}), 136.7 (C^{Mes}), 129.9 (CH^{OPh}), 129.8 (CH^{Mes}), 122.8 (CH^{imidazole}), 122.6 (CH^{imidazole}), 121.3 (CH^{OPh}), 115.3 (CH^{OPh}), 67.9 (CH₂CH₂OPh), 51.0 (CH₂CH₂OPh), 21.1 (CH₃^{p-Mes}), 20.5 (CH₃^{o-Mes}). *Syn*-form: ¹H NMR (300 MHz, C₆D₆) δ: 7.14–7.04 (m, 2H, CH^{OPh}), 6.99–6.76 (m, 8H, CH^{OPh}), 6.84 (s, 4H, CH^{Mes}), 6.50–6.43 (m, 2H, CH^{imidazole}), 5.85 (d, ³J = 1.6 Hz, 2H, CH^{imidazole}), 5.51 (t, ³J = 5.8 Hz, 4H, CH₂CH₂OPh), 4.79 (t, ³J = 5.7 Hz, 4H, CH₂CH₂OPh), 2.38 (s, 12H, CH₃^{o-Mes}), 2.15 (s, 6H, CH₃^{p-Mes}). ¹³C{¹H} NMR (101 MHz, C₆D₆) δ: 171.9 (C^{carbene}), 159.1 (C^{OPh}), 137.5 (C^{Mes}), 136.6 (C^{Mes}), 136.3 (C^{Mes}), 129.6 (CH^{OPh}), 129.3 (CH^{Mes}), 123.3 (CH^{imidazole}), 122.2 (CH^{imidazole}), 121.4 (CH^{OPh}), 115.2 (CH^{OPh}), 67.7 (CH₂CH₂OPh), 50.9 (CH₂CH₂OPh), 21.4 (CH₃^{p-Mes}), 19.9 (CH₃^{o-Mes}). MS (ESI): *m/z* 751.19 [M – Br]⁺. FTIR: $\nu_{\text{max}}(\text{solid})/\text{cm}^{-1}$ 3165w, 3137w, 2943m, 1496m, 1458m, 1439m, 1411m, 1380m, 1363m, 1347w, 1291m, 1266m, 1242m, 1226m, 1199m, 1176m, 1152m, 1115w, 1085m, 1058m, 1032m, 967vw, 934w, 906m, 881m, 867m, 853m, 790m, 751m, 689s, 642m, 592m, 571w, 509m, 486m, 467vw, 450vw, 385w, 352w, 321m, 283vw, 199s. Anal. Calcd for C₄₀H₄₄Br₂N₄NiO₂: C, 57.79; H, 5.34; N, 6.74. Found: C, 57.74; H, 5.17; N, 6.70.

Preparation of [NiBr₂{ImDiPP(C₂SPh)}₂] (19). A procedure similar to that used for compound **8** gave **19** as a pink solid (0.150 g, 62%). *Anti*-form: ¹H NMR (500 MHz, C₆D₆) δ: 7.42–7.35 (m, 2H, CH^{p-Ar}), 7.33 (d, ³J = 7.4 Hz, 4H, CH^{m-Ar}), 7.29–7.24 (m, 4H, CH^{SPh}), 7.08–7.01 (m, 6H, CH^{SPh}), 6.29 (d, ³J = 1.8 Hz, 2H, CH^{imidazole}), 6.26 (d, ³J = 1.8 Hz, 2H, CH^{imidazole}), 4.94 (t, ³J = 6.2 Hz, 4H, CH₂CH₂SPh), 3.70 (t, ³J = 6.2 Hz, 4H, CH₂CH₂SPh), 3.21 (sept, ³J = 6.7 Hz, 4H, CH^{iPr}), 1.55 (d, ³J = 6.6 Hz, 12H, CH₃^{iPr}), 0.91 (d, ³J = 6.9 Hz, 12H, CH₃^{iPr}). ¹³C{¹H} NMR (126 MHz, C₆D₆) δ: 172.8 (C^{carbene}), 148.2 (C^{DiPP}), 136.7 (C^{SPh}), 136.2 (C^{DiPP}), 130.4 (CH^{DiPP}), 129.4 (CH^{SPh}), 128.4 (CH^{SPh}), 126.0 (CH^{SPh}), 124.5 (CH^{imidazole}), 124.2 (CH^{DiPP}), 121.6 (CH^{imidazole}), 50.7 (CH₂CH₂SPh), 33.8 (CH₂CH₂SPh), 28.9 (CH^{iPr}), 26.9 (CH₃^{iPr}), 23.3 (CH₃^{iPr}). *Syn*-form: ¹H NMR (500 MHz, C₆D₆) δ: 7.42–7.34 (m, 6H, CH^{p-Ar} + CH^{m-Ar}), 7.15 (m, 4H, CH^{SPh}), 6.97–6.90 (m, 6H, CH^{SPh}), 6.28 (d, ³J = 1.8 Hz, 2H, CH^{imidazole}), 6.20 (d, ³J = 1.8 Hz, 2H, CH^{imidazole}), 5.59 (t, ³J = 7.0 Hz, 4H, CH₂CH₂SPh), 4.04 (t, ³J = 7.0 Hz, 4H, CH₂CH₂SPh), 2.96 (sept, ³J = 13.5, 6.7 Hz, 4H, CH^{iPr}), 1.23 (d, ³J = 6.6 Hz, 12H, CH₃^{iPr}), 0.90 (d, ³J = 6.8 Hz, 12H, CH₃^{iPr}). ¹³C{¹H} NMR (126 MHz, C₆D₆) δ: 171.7 (C^{carbene}), 147.1 (C^{DiPP}), 136.3 (C^{SPh}), 135.9 (C^{DiPP}), 129.9 (CH^{DiPP}), 129.6 (CH^{SPh}), 129.2 (CH^{SPh}), 126.3 (CH^{SPh}), 124.9 (CH^{imidazole}), 124.3 (CH^{DiPP}), 121.1 (CH^{imidazole}), 50.9 (CH₂CH₂SPh), 34.2 (CH₂CH₂SPh), 28.5 (CH^{iPr}), 26.7 (CH₃^{iPr}), 23.4 (CH₃^{iPr}). MS (ESI): *m/z* 867.24 [M – Cl]⁺. FTIR: $\nu_{\text{max}}(\text{solid})/\text{cm}^{-1}$ 3137w, 3072w, 2966m, 2927m, 2866m, 1458m, 1445m, 1411m, 1397m, 1377m, 1353m, 1298vw, 1275w, 1251m, 1230m, 1198m, 1178m, 1121m, 1106w, 1059m, 1015w, 957m, 934m, 883m, 802m, 748m, 761s, 733m, 709s, 690s, 643w, 612w, 565m, 486m, 461w, 361w, 208w. Anal. Calcd for C₄₆H₅₆Br₂N₄NiS₂: C, 58.30; H, 5.96; N, 5.91. Found: C, 57.93; H, 6.05; N, 5.77.

Preparation of [NiBr₂{ImDiPP(*n*-Bu)}₂] (20). A procedure similar to that used for compound **8** gave **20** as a pink solid. The product was recrystallized from hot THF to afford **20** as a pink powder (0.288 g, 88%). *Anti*-form: ¹H NMR (300 MHz, C₆D₆) δ: 7.47–7.29 (m, 6H, CH^{p-Ar} + CH^{m-Ar}), 6.38 (d, ³J = 1.9 Hz, 2H, CH^{imidazole}), 6.18 (d, ³J = 1.9 Hz, 2H, CH^{imidazole}), 4.80 (t, ³J = 7.8 Hz, 4H, CH₂CH₂CH₂CH₃), 3.31 (sept, ³J = 6.7 Hz, 4H, CH^{iPr}), 1.91–1.73 (m, 4H, CH₂CH₂CH₂CH₃), 1.58 (d, ³J = 6.6 Hz, 12H, CH₃^{iPr}), 1.23–1.10 (m, 2H, CH₂CH₂CH₂CH₃), 0.97 (d, ³J = 6.9 Hz, 12H, CH₃^{iPr}), 0.87 (t, ³J = 7.3 Hz, 6H, CH₂CH₂CH₂CH₃). ¹³C{¹H} NMR (126 MHz, C₆D₆) δ: 172.6 (C^{carbene}), 148.3 (C^{Ar}), 136.6 (C^{Ar}), 130.1 (CH^{Ar}), 124.9 (CH^{imidazole}), 124.0 (CH^{Ar}), 119.7 (CH^{imidazole}), 51.5 (CH₂CH₂CH₂CH₃), 32.4 (CH₂CH₂CH₂CH₃), 28.9 (CH^{iPr}), 26.9 (CH₃^{iPr}), 23.4 (CH₃^{iPr}), 20.4 (CH₂CH₂CH₂CH₃), 14.2

(CH₂CH₂CH₂CH₃). *Syn*-form: ¹H NMR (300 MHz, C₆D₆) δ: 7.45–7.30 (m, 2H, CH^{*p*-Ar}), 7.20–7.16 (m, 4H, CH^{*m*-Ar}), 6.33 (d, ³J = 1.9 Hz, 2H, CH^{imidazole}), 6.26 (d, ³J = 1.9 Hz, 2H, CH^{imidazole}), 5.45 (t, ³J = 7.8 Hz, 4H, CH₂CH₂CH₂CH₃), 3.05 (sept, ³J = 6.7 Hz, 4H, CH^{iPr}), 2.18–2.02 (m, 4H, CH₂CH₂CH₂CH₃), 1.56–1.44 (m, 4H, CH₂CH₂CH₂CH₃), 1.24 (d, ³J = 6.7 Hz, 12H, CH₃^{iPr}), 1.01–0.91 (m, 18H, CH₃^{iPr} + CH₂CH₂CH₂CH₃). ¹³C{¹H} NMR (126 MHz, C₆D₆) δ: 171.6 (C^{carbene}), 147.3 (C^{Ar}), 136.3 (C^{Ar}), 129.8 (CH^{Ar}), 125.1 (CH^{imidazole}), 124.3 (CH^{Ar}), 119.6 (CH^{imidazole}), 51.6 (CH₂CH₂CH₂CH₃), 32.8 (CH₂CH₂CH₂CH₃), 28.6 (CH^{iPr}), 26.7 (CH₃^{iPr}), 23.5 (CH₃^{iPr}), 20.9 (CH₂CH₂CH₂CH₃), 14.2 (CH₂CH₂CH₂CH₃). MS (ESI): *m/z* 707.30 [M – Br]⁺. FTIR: ν_{max}(solid)/cm^{–1} 3132vw, 2955w, 2868w, 1466m, 1456m, 1414m, 1395m, 1382m, 1361m, 1319vw, 1296w, 1275w, 1266w, 1254w, 1222m, 1197m, 119m, 1080vw, 1059m, 958m, 932m, 883vw, 800m, 760s, 735m, 706s, 647vw, 618vw, 571m, 478m, 457w, 423vw, 376w, 354m, 345m, 322w, 284m. Anal. Calcd for C₃₈H₅₆Br₂N₄Ni: C, 57.97; H, 7.17; N, 7.12. Found: C, 57.90; H, 7.24; N, 6.90.

Preparation of [NiL₂{ImDiPP(C₂OMe)}₂] (21). To a solution of the nickel complex 5 (0.200 g, 0.285 mmol) in acetone (10 mL) was added solid KI (0.127 g, 0.765 mmol). The reaction mixture turned immediately dark blue-purple and was stirred for 3 h at room temperature. The solvent was removed under reduced pressure, and the dark residue was solubilized in benzene. The white precipitate (KCl) was filtered off the dark blue-purple solution by filtration through Celite, and the solvent was removed under reduced pressure to yield 21 as a dark powder (0.250 g, 99%). *Syn*-form: ¹H NMR (C₆D₆, 500 MHz) δ: 7.34–7.29 (m, 2H, CH^{*p*-Ar}), 7.11 (d, ³J = 7.8 Hz, 4H, CH^{*m*-Ar}), 6.85 (d, ³J = 1.8 Hz, 2H, CH^{imidazole}), 6.37 (d, ³J = 1.8 Hz, 2H, CH^{imidazole}), 5.58 (t, ³J = 5.2 Hz, 4H, CH₂CH₂OMe), 4.04 (t, ³J = 5.2 Hz, 4H, CH₂CH₂OMe), 3.16 (sept, ³J = 6.7 Hz, 4H, CH^{iPr}), 3.05 (s, 6H, CH₃^{OMe}), 1.26 (d, ³J = 6.7 Hz, 12H, CH₃^{iPr}), 0.88 (d, ³J = 6.8 Hz, 12H, CH₃^{iPr}). ¹³C{¹H} NMR (C₆D₆, 126 MHz) δ: 175.4 (C^{carbene}), 147.1 (C^{Ar}), 135.8 (C^{Ar}), 129.9 (CH^{Ar}), 126.4 (CH^{imidazole}), 124.5 (CH^{Ar}), 121.9 (CH^{imidazole}), 71.2 (CH₂CH₂OMe), 58.6 (CH₃^{OMe}), 52.5 (CH₂CH₂OMe), 28.8 (CH^{iPr}), 26.7 (CH₃^{iPr}). *Anti*-form: ¹H NMR (C₆D₆, 500 MHz) δ: 7.34–7.29 (m, 2H, CH^{*p*-Ar}), 7.26 (d, ³J = 6.7 Hz, 4H, CH^{*m*-Ar}), 6.81 (d, ³J = 1.8 Hz, 2H, CH^{imidazole}), 6.43 (d, ³J = 1.9 Hz, 2H, CH^{imidazole}), 5.01 (t, ³J = 4.9 Hz, 4H, CH₂CH₂OMe), 3.72 (t, ³J = 4.9 Hz, 4H, CH₂CH₂OMe), 3.48 (sept, ³J = 6.7 Hz, 4H, CH^{iPr}), 2.97 (s, 2H, CH₃^{OMe}), 1.59 (d, ³J = 6.6 Hz, 12H, CH₃^{iPr}), 0.91 (d, ³J = 6.8 Hz, 12H, CH₃^{iPr}). ¹³C{¹H} NMR (C₆D₆, 126 MHz) δ: 175.7 (C^{carbene}), 148.2 (C^{Ar}), 136.3 (C^{Ar}), 130.2 (CH^{Ar}), 126.1 (CH^{imidazole}), 124.2 (CH^{Ar}), 122.2 (CH^{imidazole}), 71.1 (CH₂CH₂OMe), 58.4 (CH₃^{OMe}), 52.2 (CH₂CH₂OMe), 29.2 (CH^{iPr}), 26.9 (CH₃^{iPr}), 23.8 (CH₃^{iPr}). MS (ESI): *m/z* 757.24 [M – Br]⁺. FTIR: ν_{max}(solid)/cm^{–1} 3123w, 2961m, 2928m, 2866m, 1459m, 1443m, 1406m, 1381m, 1359m, 1328w, 1263m, 1234w, 1207m, 1176w, 1119s, 1084w, 1071w, 1034m, 1012w, 978w, 948w, 934w, 886vw, 830w, 801m, 758s, 706s, 677w, 648w, 633w, 592m, 565m, 546w, 526w, 468m, 420vw. Anal. Calcd for C₃₆H₅₂I₂N₄NiO₂: C, 48.84; H, 5.92; N, 6.33. Found: C, 48.80; H, 5.91; N, 6.32.

Preparation of [NiL₂{ImMes(C₂OMe)}₂] (22). A procedure similar to that used for compound 21 gave 22 as a dark solid (0.314 mg, 97%). *Syn*-form: ¹H NMR (500 MHz, C₆D₆) δ: 6.78 (s, 4H, CH^{Mes}), 6.76 (d, ³J = 1.8 Hz, 2H, CH^{imidazole}), 5.89 (d, ³J = 1.7 Hz, 2H, CH^{imidazole}), 5.36 (t, ³J = 5.2 Hz, 4H, CH₂CH₂OMe), 4.01 (t, ³J = 5.2 Hz, 4H, CH₂CH₂OMe), 3.07 (s, 6H, CH₃^{OMe}), 2.35 (s, 6H, CH₃^{p-Mes}), 2.22 (s, 12H, CH₃^{o-Mes}). ¹³C{¹H} NMR (126 MHz, C₆D₆) δ: 174.8 (C^{carbene}), 137.5 (C^{Mes}), 136.4 (C^{Mes}), 136.2 (C^{Mes}), 129.8 (CH^{Mes}), 124.7 (CH^{imidazole}), 122.6 (CH^{imidazole}), 71.4 (CH₂CH₂OMe), 58.6 (CH₃^{OMe}), 52.2 (CH₂CH₂OMe), 21.6 (CH₃^{o-Mes}), 21.4 (CH₃^{p-Mes}). *Anti*-form: ¹H NMR (500 MHz, C₆D₆) δ: 6.87 (s, 4H, CH^{Mes}), 6.66 (d, ³J = 1.8 Hz, 2H, CH^{imidazole}), 5.93 (d, ³J = 1.7 Hz, 2H, CH^{imidazole}), 4.93 (t, ³J = 4.9 Hz, 4H, CH₂CH₂OMe), 3.86 (t, ³J = 4.9 Hz, 4H, CH₂CH₂OMe), 3.06 (s, 6H, CH₃^{OMe}), 2.48 (s, 12H, CH₃^{o-Mes}), 2.19 (s, 6H, CH₃^{p-Mes}). ¹³C{¹H} NMR (126 MHz, C₆D₆) δ: 174.5 (C^{carbene}), 138.3 (C^{Mes}), 137.2 (C^{Mes}), 136.8 (C^{Mes}), 129.5 (CH^{Mes}), 124.1 (CH^{imidazole}), 123.1 (CH^{imidazole}), 71.2 (CH₂CH₂OMe), 58.5 (CH₃^{OMe}), 51.9 (CH₂CH₂OMe), 22.5 (CH₃^{o-Mes}), 21.1 (CH₃^{p-Mes}).

MS (ESI): *m/z* 673.15 [M – I]⁺. FTIR: ν_{max}(solid)/cm^{–1} 3144w, 2917m, 1486m, 1439m, 1408m, 1376m, 1347m, 1333m, 1288w, 1260w, 1234w, 1215m, 1191w, 1116s, 1080m, 1034m, 1007m, 973m, 931m, 852m, 834m, 738m, 702s, 647w, 585m, 551vw, 511w, 452w, 333w, 281m, 195m. Anal. Calcd for C₃₀H₄₀I₂N₄NiO₂: C, 44.98; H, 5.03; N, 6.99. Found: C, 45.05; H, 5.05; N, 6.98.

Preparation of [NiL₂{Imn-Bu(C₂OMe)}₂] (23). A procedure similar to that used for compound 21 gave 23 as a dark solid (0.086 g, 91%). Most signals of both conformers (*syn*- and *anti*-forms) are superimposed: ¹H NMR (400 MHz, C₆D₆) δ: 6.65–6.61 (m, 2H, CH^{imidazole}), 6.18–6.12 (m, 2H, CH^{imidazole}), 5.10–5.00 (m, 4H, CH₂CH₂OMe), 4.74–4.64 (m, 4H, CH₂CH₂CH₂CH₃^{nBu}), 4.11–3.99 (m, 4H, CH₂CH₂OMe), 3.10 (s, 3H, CH₃^{OMe}), 3.09 (s, 3H, CH₃^{OMe}), 2.13–1.96 (m, 4H, CH₂CH₂CH₂CH₃^{nBu}), 1.54–1.31 (m, 4H, CH₂CH₂CH₂CH₃^{nBu}), 1.01–0.91 (m, 6H, CH₂CH₂CH₂CH₃^{nBu}). ¹³C{¹H} NMR (101 MHz, C₆D₆) δ: 174.8 (C^{carbene}), 174.7 (C^{carbene}), 123.1 (CH^{imidazole}), 123.1 (CH^{imidazole}), 121.1 (CH^{imidazole}), 121.0 (CH^{imidazole}), 71.3 (CH₂CH₂OMe), 71.2 (CH₂CH₂OMe), 58.7 (CH₃^{OMe}), 58.7 (CH₃^{OMe}), 51.2 (CH₂CH₂OMe), 51.1 (CH₂CH₂OMe), 51.0 (CH₂CH₂CH₂CH₃^{nBu}), 51.0 (CH₂CH₂CH₂CH₃^{nBu}), 32.1 (CH₂CH₂CH₂CH₃^{nBu}), 32.0 (CH₂CH₂CH₂CH₃^{nBu}), 20.6 (CH₂CH₂CH₂CH₃^{nBu}), 20.5 (CH₂CH₂CH₂CH₃^{nBu}), 14.1 (CH₃^{nBu}), 14.0 (CH₃^{nBu}). MS (ESI): *m/z* 549.12 [M – I]⁺. FTIR: ν_{max}(solid)/cm^{–1} 3159w, 3126w, 2958m, 2929m, 2870m, 2830m, 2810m, 1446m, 1416m, 1371m, 1344m, 1296w, 1273m, 1223m, 1198m, 1177m, 1113s, 1098m, 1085m, 1036m, 1004m, 967m, 933w, 906w, 831m, 801w, 763m, 736m, 698s, 633w, 613w, 556w, 536m, 468m, 439m, 372w, 324m, 306m, 212m, 118m. Anal. Calcd for C₂₀H₃₆I₂N₄NiO₂: C, 35.48; H, 5.36; N, 8.28. Found: C, 35.41; H, 5.48; N, 8.09.

Preparation of *cis*-[Ni{ImMes(C₂OMe)}₂(H₂O)₂][PF₆]₂ (27). To a solution of the nickel complex 9 (0.328 g, 0.464 mmol) in THF (10 mL) containing a few drops of water was added TIPF₆ (0.366 g, 1.05 mmol). The reaction mixture turned immediately yellow, a white precipitate formed, and stirring was maintained for 16 h at room temperature. The solvent was evaporated under reduced pressure, and the yellow residue was solubilized in MeCN. The white precipitate (TlCl) was filtered off, and the solvent was removed under reduced pressure. The yellow residue was triturated with pentane until a yellow powder was obtained to yield 27 (0.336 g, 84%). ¹H NMR (CD₃CN, 300 MHz): δ 7.44 (d, ³J = 2.1 Hz, 2H, CH^{imidazole}), 7.38 (s, 2H, CH^{Mes}), 7.17 (s, 2H, CH^{Mes}), 7.11 (d, ³J = 2.0 Hz, 2H, CH^{imidazole}), 4.49–4.39 (m, 2H, CH₂CH₂OMe), 3.63–3.53 (m, 2H, CH₂CH₂OMe), 3.49–3.38 (m, 2H, CH₂CH₂OMe), 3.28 (s, 6H, CH₃^{OMe}), 3.18–3.06 (m, 2H, CH₂CH₂OMe), 2.47 (s, 6H, CH₃^{p-Mes}), 2.14 (s, 6H, CH₃^{o-Mes}), 1.41 (s, 6H, CH₃^{o-Mes}). ¹³C{¹H} NMR (126 MHz, CD₃CN): δ 147.7 (C^{carbene}), 141.8 (C^{Mes}), 138.0 (C^{Mes}), 135.5 (C^{Mes}), 134.6 (C^{Mes}), 131.4 (CH^{Mes}), 131.2 (CH^{Mes}), 127.9 (CH^{imidazole}), 125.1 (CH^{imidazole}), 70.7 (CH₂CH₂OMe), 59.3 (CH₃^{OMe}), 49.9 (CH₂CH₂OMe), 21.1 (CH₃^{p-Mes}), 18.6 (CH₃^{o-Mes}), 18.1 (CH₃^{o-Mes}). FTIR: ν_{max}(solid)/cm^{–1} 3145w, 2936w, 1653w, 1609w, 1487m, 1488m, 1420m, 1242m, 1213m, 115m, 1076m, 1011w, 820s, 738m, 712m, 695m. Anal. Calcd for C₃₀H₄₄F₁₂N₄NiO₄P₂: C, 41.26; H, 5.08; N, 6.42. Found: C, 41.03; H, 5.27; N, 6.25.

Preparation of *cis*-[Ni{ImDiPP(*n*-Bu)}₂(H₂O)₂][PF₆]₂ (28). A procedure similar to that used for compound 27 gave 28 as a yellow powder (0.273 g, 91%). ¹H NMR (CD₃CN, 300 MHz): δ 7.79–7.74 (m, 4H, CH^{*m*-Ar}), 7.51–7.45 (m, 2H, CH^{*p*-Ar}), 7.33 (d, ³J = 2.0 Hz, 2H, CH^{imidazole}), 7.29 (d, ³J = 2.0 Hz, 2H, CH^{imidazole}), 4.11–3.95 (m, 2H, CH₂CH₂CH₂CH₃), 2.89 (ddd, ³J = 13.7, 11.8, 5.3 Hz, 2H, CH₂CH₂CH₂CH₃), 2.60 (sept, ³J = 6.8 Hz, 2H, CH^{iPr}), 2.13 (s, 2H, H₂O), 1.73 (d, ³J = 6.8 Hz, 6H, CH₃^{iPr}), 1.80–1.61 (m, 6H, CH₂CH₂CH₂CH₃ + CH^{iPr}), 1.52–1.38 (m, 2H, CH₂CH₂CH₂CH₃), 1.24–1.36 (m, 4H, CH₂CH₂CH₂CH₃), 1.06 (d, ³J = 6.7 Hz, 6H, CH₃^{iPr}), 1.05 (d, ³J = 6.7 Hz, 6H, CH₃^{iPr}), 0.97 (t, ³J = 7.3 Hz, 6H, CH₂CH₂CH₂CH₃), 0.73 (d, ³J = 6.9 Hz, 6H, CH₃^{iPr}). ¹³C{¹H} NMR (75 MHz, CD₃CN) δ 148.5 (C^{Ar}), 146.5 (C^{Ar}), 145.0 (C^{carbene}), 134.3 (C^{Ar}), 132.8 (CH^{Ar}), 129.9 (CH^{imidazole}), 126.6 (CH^{Ar}), 126.4 (CH^{Ar}), 124.6 (CH^{imidazole}), 49.9 (CH₂CH₂CH₂CH₃), 31.7 (CH₂CH₂CH₂CH₃), 29.4 (CH^{iPr}), 29.2 (CH^{iPr}), 26.6 (CH₃^{iPr}), 26.3

(CH₃^{iPr}), 24.0 (CH₃^{iPr}), 22.6 (CH₃^{iPr}), 20.6 (CH₂CH₂CH₂CH₃), 13.9 (CH₂CH₂CH₂CH₃). FTIR: $\nu_{\text{max}}(\text{solid})/\text{cm}^{-1}$ 3183w, 2968m, 2937w, 2873w, 1463m, 1419m, 1388m, 1368m, 1303w, 1220m, 1123w, 1058w, 955w, 830s, 768m, 740m, 723w, 105m. Anal. Calcd for C₃₈H₆₀F₁₂N₄NiO₂P₂: C, 47.87; H, 6.34; N, 5.88. Found: C, 48.15; H, 6.09; N, 6.12.

Catalytic Oligomerization of Ethylene. The catalytic reactions were performed in a magnetically stirred (1200 rpm) 145 mL stainless steel autoclave. A 125 mL glass container was used to avoid corrosion of the autoclave walls. The precatalyst solution was prepared by dissolving 4×10^{-5} mol of a powder of the complex [(1-H)₂(NiCl₄)]_{5–10}, 18–23, and 27–29 in toluene or chlorobenzene (10 mL). AlEtCl₂ (EADC) or MAO was used as cocatalyst (5 mL of a 8×10^{-5} mol toluene solution or 10.66 mL of a 1.5×10^{-3} mol toluene solution, respectively). The precatalyst solution (10 mL) was injected into the reactor under an ethylene flux, followed by the cocatalyst solution (10 or 400 equiv for EADC or MAO, respectively, in 5 mL of toluene, total volume of the solution: 15 mL). The catalytic reaction was started at 20 °C, unless otherwise specified. No cooling of the reactor was done during the reaction. After injection of the catalyst and cocatalyst solutions under a constant low flow of ethylene, which is considered as the t_0 time, the reactor was immediately pressurized to 10 bar of ethylene. The temperature increased, owing solely to the exothermicity of the reaction. The 10 bar working pressure was maintained through a continuous feed of ethylene from a bottle placed on a balance to allow continuous monitoring of the ethylene uptake. At the end of each test (35 min), a dry ice bath was used to rapidly cool the reactor. When the inner temperature reached 0 °C, the ice bath was removed, allowing the temperature to slowly rise to 18 °C. The gaseous phase was then transferred into a 10 L polyethylene tank filled with water. An aliquot of this gaseous phase was transferred into a Schlenk flask, previously evacuated, for GC analysis. The amount of ethylene consumed was thus determined by differential weighting of the bottle (accuracy of the scale: 0.1 g). To this amount of ethylene, the remaining ethylene (calculated using the GC analysis) in the gaseous phase was subtracted. Although this method is of limited accuracy, it was used throughout and gave satisfactory reproducibility. The reaction mixture in the reactor was quenched *in situ* by the addition of ethanol (1 mL), transferred into a Schlenk flask, and separated from the metal complexes by trap-to-trap evaporation (20 °C, 0.8 mbar) into a second Schlenk flask previously immersed in liquid nitrogen in order to avoid loss of product for GC analysis. Each catalytic test was performed at least twice to ensure the reproducibility of the results.

■ ASSOCIATED CONTENT

Supporting Information

NMR data, mass spectra analyses, and ORTEP views. Crystal data of [(1-H)₂(NiCl₄)]_{6–12}, 18–23, and 27 are available. The crystallographic information files (CIF) have been deposited with the CCDC, 12 Union Road, Cambridge, CB2 1EZ, U.K., and can be obtained on request free of charge, by quoting the publication citation and deposition numbers 985601–985613, 1015661, and 1015662. This material is available free of charge via the Internet at <http://pubs.acs.org>.

■ AUTHOR INFORMATION

Corresponding Author

*E-mail: braunstein@unistra.fr.

Notes

The authors declare no competing financial interest.

■ ACKNOWLEDGMENTS

The Centre National de la Recherche Scientifique (CNRS), the Ministère de l'Enseignement Supérieur et de la Recherche (Ph.D. fellowship to S.H.), and the IFP Energies nouvelles (IFPEN) are gratefully acknowledged for support. We are

grateful to Dr. C. Fliedel for providing a sample of 1-(2,6-diisopropylphenyl)-3-(2-(phenylthio)ethyl)-1H-imidazol-3-ium chloride ([([ImH]DiPP(C₂SPh))Cl, 16·HCl) and to Mélanie Boucher and Marc Mermillon-Fournier for experimental support. The NMR service of the Université de Strasbourg is warmly acknowledged for the 2D correlation experiments.

■ REFERENCES

- (1) (a) Herrmann, W. A.; Köcher, C. *Angew. Chem., Int. Ed. Engl.* **1997**, *36*, 2162. (b) Bourissou, D.; Guerret, O.; Gabbai, F. P.; Bertrand, G. *Chem. Rev.* **2000**, *100*, 39. (c) Herrmann, W. A. *Angew. Chem., Int. Ed.* **2002**, *41*, 1290. (d) Crudden, C. M.; Allen, D. P. *Coord. Chem. Rev.* **2004**, *248*, 2247. (e) Hahn, F. E. *Angew. Chem., Int. Ed.* **2006**, *45*, 1348. (f) Pugh, D.; Danopoulos, A. A. *Coord. Chem. Rev.* **2007**, *251*, 610. (g) Hahn, F.; Jahnke, M. *Angew. Chem., Int. Ed.* **2008**, *47*, 3122. (h) de Frémont, P.; Marion, N.; Nolan, S. P. *Coord. Chem. Rev.* **2009**, *253*, 862. (i) Díez-González, S.; Marion, N.; Nolan, S. P. *Chem. Rev.* **2009**, *109*, 3612. (j) Gusev, D. G. *Organometallics* **2009**, *28*, 763. (k) Jacobsen, H.; Correa, A.; Poater, A.; Costabile, C.; Cavallo, L. *Coord. Chem. Rev.* **2009**, *253*, 687. (l) *N-Heterocyclic Carbenes in Transition Metal Catalysis and Organocatalysis*; Cazin, C. S. J., Ed.; Springer, 2011.
- (2) Díez-González, S.; Marion, N.; Nolan, S. P. *Chem. Rev.* **2009**, *109*, 3612.
- (3) (a) Köhl, O. *Chem. Soc. Rev.* **2007**, *36*, 592. (b) Liddle, S. T.; Edworthy, I. S.; Arnold, P. L. *Chem. Soc. Rev.* **2007**, *36*, 1732.
- (4) (a) Peris, E.; Crabtree, R. H. *Coord. Chem. Rev.* **2004**, *248*, 2239. (b) Pugh, D.; Danopoulos, A. A. *Coord. Chem. Rev.* **2007**, *251*, 610. (c) Fliedel, C.; Braunstein, P. J. *Organomet. Chem.* **2014**, *751*, 286.
- (5) (a) McGuinness, D. S.; Gibson, V. C.; Wass, D. F.; Steed, J. W. J. *Am. Chem. Soc.* **2003**, *125*, 12716. (b) McGuinness, D. S.; Gibson, V. C.; Steed, J. W. *Organometallics* **2004**, *23*, 6288. (c) McGuinness, D. S.; Suttill, J. A.; Gardiner, M. G.; Davies, N. W. *Organometallics* **2008**, *27*, 4238. (d) McGuinness, D. S. *Organometallics* **2009**, *28*, 244. (e) Al Thagfi, J.; Lavoie, G. G. *Organometallics* **2012**, *31*, 2463.
- (6) (a) Csabai, P.; Joó, F.; Trzeciak, A. M.; Ziolkowski, J. J. *J. Organomet. Chem.* **2006**, *691*, 3371. (b) Diver, S. T.; Kulkarni, A. A.; Clark, D. A.; Peppers, B. P. *J. Am. Chem. Soc.* **2007**, *129*, 5832.
- (7) (a) McGuinness, D. S.; Mueller, W.; Wasserscheid, P.; Cavell, K. J.; Skelton, B. W.; White, A. H.; Englert, U. *Organometallics* **2002**, *21*, 175. (b) MacKinnon, A. L.; Baird, M. C. *J. Organomet. Chem.* **2003**, *683*, 114. (c) Sun, H. M.; Shao, Q.; Hu, D. M.; Li, W. F.; Shen, Q.; Zhang, Y. *Organometallics* **2005**, *24*, 331. (d) Li, W.-F.; Sun, H.-M.; Chen, M.-Z.; Shen, Q.; Zhang, Y. *J. Organomet. Chem.* **2008**, *693*, 2047. (e) Benítez Junquera, L.; Puerta, M. C.; Valerga, P. *Organometallics* **2012**, *31*, 2175. (f) Hameury, S.; de Frémont, P.; Breuil, P.-A. R.; Olivier-Bourbigou, H.; Braunstein, P. *Dalton Trans.* **2014**, *43*, 4700. (g) Hameury, S.; de Frémont, P.; Breuil, P.-A. R.; Olivier-Bourbigou, H.; Braunstein, P. *Inorg. Chem.* **2014**, *5189*.
- (8) Dagnone, S.; Bellemin-Lapponnaz, S.; Romain, C. *Organometallics* **2013**, *32*, 2736.
- (9) Gil, W.; Lis, T.; Trzeciak, A. M.; Ziolkowski, J. J. *Inorg. Chim. Acta* **2006**, *359*, 2835.
- (10) Khlebnikov, V.; Meduri, A.; Mueller-Bunz, H.; Montini, T.; Fornasiero, P.; Zangrando, E.; Milani, B.; Albrecht, M. *Organometallics* **2012**, *31*, 976.
- (11) (a) Skupinska, J. *Chem. Rev.* **1991**, *91*, 613. (b) Killian, C. M.; Johnson, L. K.; Brookhart, M. *Organometallics* **1997**, *16*, 2005. (c) Ittel, S. D.; Johnson, L. K.; Brookhart, M. *Chem. Rev.* **2000**, *100*, 1169. (d) Mecking, S. *Angew. Chem., Int. Ed.* **2001**, *40*, 534. (e) Gibson, V. C.; Spitzmesser, S. K. *Chem. Rev.* **2003**, *103*, 283. (f) Dixon, J. T.; Green, M. J.; Hess, F. M.; Morgan, D. H. *J. Organomet. Chem.* **2004**, *689*, 3641. (g) Lappin, G. R.; Nemeec, L. H.; Sauer, J. D.; Wagner, J. D. Higher Olefins. In *Kirk-Othmer Encyclopedia of Chemical Technology*, 2005. (h) Bianchini, C.; Giambastiani, G.; Rios, I. G.; Mantovani, G.; Meli, A.; Segarra, A. M. *Coord. Chem. Rev.* **2006**, *250*, 1391. (i) Forestière, A.; Olivier-Bourbigou, H.; Saussine, L. *Oil Gas Sci. Technol.* **2009**, *64*, 649. (j) Bianchini, C.; Giambastiani, G.; Luconi, L.

- Meli, A. *Coord. Chem. Rev.* **2010**, 254, 431. (k) Rhinehart, J. L.; Brown, L. A.; Long, B. K. *J. Am. Chem. Soc.* **2013**, 135, 16316. (l) Keim, W. *Angew. Chem., Int. Ed.* **2013**, 52, 12492. (m) Wang, S.; Sun, W.-H.; Redshaw, C. *J. Organomet. Chem.* **2014**, 751, 717. (n) Speiser, F.; Braunstein, P.; Saussine, L. *Acc. Chem. Res.* **2005**, 38, 784.
- (12) Fischer, K.; Jonas, K.; Misbach, P.; Stabba, R.; Wilke, G. *Angew. Chem., Int. Ed. Engl.* **1973**, 12, 943.
- (13) Kermagoret, A.; Braunstein, P. *Dalton Trans.* **2008**, 822.
- (14) Cavell, K. J.; McGuinness, D. S. *Coord. Chem. Rev.* **2004**, 248, 671.
- (15) (a) Ketz, B. E.; Ottenwaelder, X. G.; Waymouth, R. M. *Chem. Commun.* **2005**, 5693. (b) Benson, S.; Payne, B.; Waymouth, R. M. *J. Polym. Sci., Part A: Polym. Chem.* **2007**, 45, 3637. (c) Kong, Y.; Cheng, M.; Ren, H.; Xu, S.; Song, H.; Yang, M.; Liu, B.; Wang, B. *Organometallics* **2011**, 30, 1677. (d) Song, H.; Fan, D.; Liu, Y.; Hou, G.; Zi, G. *J. Organomet. Chem.* **2013**, 729, 40. (e) Li, W.; Sun, H.; Chen, M.; Wang, Z.; Hu, D.; Shen, Q.; Zhang, Y. *Organometallics* **2005**, 24, 5925.
- (16) Braunstein, P.; Naud, F. *Angew. Chem., Int. Ed.* **2001**, 40, 680.
- (17) (a) Speiser, F.; Braunstein, P.; Saussine, L. *Inorg. Chem.* **2004**, 43, 4234. (b) Speiser, F.; Braunstein, P.; Saussine, L. *Organometallics* **2004**, 23, 2633. (c) Kermagoret, A.; Braunstein, P. *Dalton Trans.* **2008**, 1564. (d) Kermagoret, A.; Braunstein, P. *Organometallics* **2008**, 27, 88. (e) Boudier, A.; Breuil, P.-A. R.; Magna, L.; Olivier-Bourbigou, H.; Braunstein, P. *J. Organomet. Chem.* **2012**, 718, 31.
- (18) (a) Zhang, X.; Qiu, Y.; Rao, B.; Luo, M. *Organometallics* **2009**, 28, 3093. (b) Özdemir, I.; Gök, Y.; Özeroğlu, O.; Kaloğlu, M.; Doucet, H.; Bruneau, C. *Eur. J. Inorg. Chem.* **2010**, 1798. (c) Lund, C. L.; Sgro, M. J.; Cariou, R.; Stephan, D. W. *Organometallics* **2012**, 31, 802. (d) Lund, C. L.; Sgro, M. J.; Stephan, D. W. *Organometallics* **2012**, 31, 580. (e) Villaverde, G.; Corma, A.; Iglesias, M.; Sánchez, F. *ACS Catal.* **2012**, 2, 399. (f) Doğan, O.; Kaloğlu, N.; Demir, S.; Özdemir, I.; Günel, S.; Özdemir, I. *Monatsh. Chem.* **2013**, 144, 313. (g) Türkmen, H.; Gök, L.; Kani, I.; Çetinkaya, B. *Türk. J. Chem.* **2013**, 37, 633. (h) Wang, T.; Pranckevicius, C.; Lund, C. L.; Sgro, M. J.; Stephan, D. W. *Organometallics* **2013**, 32, 2168.
- (19) (a) Çetinkaya, B.; Demir, S.; Özdemir, I.; Toupet, L.; Semeril, D.; Bruneau, C.; Dixneuf, P. H. *Chem.—Eur. J.* **2003**, 9, 2323. (b) Özdemir, I.; Demir, S.; Gök, Y.; Çetinkaya, E.; Çetinkaya, B. *J. Mol. Catal. A: Chem.* **2004**, 222, 97. (c) Özdemir, I.; Gürbüz, N.; Gök, Y.; Çetinkaya, B.; Çetinkaya, E. *Transition Met. Chem.* **2005**, 30, 367. (d) Türkmen, H.; Denizalti, S.; Özdemir, I.; Çetinkaya, E.; Çetinkaya, B. *J. Organomet. Chem.* **2008**, 693, 425. (e) Özdemir, I.; Gürbüz, N.; Doğan, O.; Günel, S.; Özdemir, I. *Appl. Organomet. Chem.* **2010**, 24, 758. (f) Özdemir, I.; Demir, S.; Günel, S.; Özdemir, I.; Arici, C.; Ülkü, D. *Inorg. Chim. Acta* **2010**, 363, 3803. (g) Gürbüz, N.; Yaşar, S.; Özcan, E. Ö.; Özdemir, I.; Çetinkaya, B. *Eur. J. Inorg. Chem.* **2010**, 3051. (h) Iglesias, M.; Pérez-Nicolás, M.; Miguel, P. J. S.; Polo, V.; Fernández-Alvarez, F. J.; Perez-Torrente, J. J.; Oro, L. A. *Chem. Commun.* **2012**, 48, 9480.
- (20) (a) Yang, X.; Fei, Z.; Geldbach, T. J.; Phillips, A. D.; Hartinger, C. G.; Li, Y.; Dyson, P. J. *Organometallics* **2008**, 27, 3971. (b) Türkmen, H.; Pape, T.; Hahn, F. E.; Çetinkaya, B. *Eur. J. Inorg. Chem.* **2008**, 5418. (c) Türkmen, H.; Pape, T.; Hahn, F. E.; Çetinkaya, B. *Eur. J. Inorg. Chem.* **2009**, 285. (d) Doğan, O.; Gürbüz, N.; Özdemir, I.; Çetinkaya, B.; Şahin, O.; Büyükgüngör, O. *Dalton Trans.* **2009**, 7087. (e) Emin, G. M.; Gümüşada, R.; Özdemir, N.; Dinçer, M.; Çetinkaya, B. *Inorg. Chem. Commun.* **2009**, 12, 990. (f) Doğan, O.; Demir, S.; Özdemir, I.; Çetinkaya, B. *Appl. Organomet. Chem.* **2011**, 25, 163. (g) Jiménez, M. V.; Fernández-Tornos, J.; Pérez-Torrente, J. J.; Modrego, F. J.; Winterle, S.; Cunchillos, C.; Lahoz, F. J.; Oro, L. A. *Organometallics* **2011**, 30, 5493. (h) Talisman, I. J.; Kumar, V.; Deschamps, J. R.; Frisch, M.; Malhotra, S. V. *Carbohydr. Res.* **2011**, 346, 2337. (i) Türkmen, H.; Pelit, L.; Çetinkaya, B. *J. Mol. Catal. A: Chem.* **2011**, 348, 88. (j) Özdemir, I.; Gürbüz, N.; Kaloğlu, N.; Doğan, O.; Kaloğlu, M.; Bruneau, C.; Doucet, H. *Beilstein J. Org. Chem.* **2013**, 9, 303.
- (21) Cariou, R.; Fischmeister, C.; Toupet, L.; Dixneuf, P. H. *Organometallics* **2006**, 25, 2126.
- (22) (a) Herrmann, W. A.; Gerstberger, G.; Spiegler, M. *Organometallics* **1997**, 16, 2209. (b) Matsubara, K.; Ueno, K.; Shibata, Y. *Organometallics* **2006**, 25, 3422. (c) Wolf, J.; Labande, A.; Daran, J.-C.; Poli, R. *Eur. J. Inorg. Chem.* **2007**, 5069. (d) Yang, W.-H.; Lee, C.-S.; Pal, S.; Chen, Y.-N.; Hwang, W.-S.; Lin, I. J. B.; Wang, J.-C. *J. Organomet. Chem.* **2008**, 693, 3729. (e) Huang, Y.-P.; Tsai, C.-C.; Shih, W.-C.; Chang, Y.-C.; Lin, S.-T.; Yap, G. P. A.; Chao, I.; Ong, T.-G. *Organometallics* **2009**, 28, 4316. (f) Liu, Z.-h.; Xu, Y.-C.; Xie, L.-Z.; Sun, H.-M.; Shen, Q.; Zhang, Y. *Dalton Trans.* **2011**, 40, 4697. (g) Shibata, T.; Ito, S.; Doe, M.; Tanaka, R.; Hashimoto, H.; Kinoshita, I.; Yano, S.; Nishioka, T. *Dalton Trans.* **2011**, 40, 6778. (h) Badaj, A. C.; Lavoie, G. G. *Organometallics* **2012**, 31, 1103. (i) Zhang, D.; Zhou, S.; Li, Z.; Wang, Q.; Weng, L. *Dalton Trans.* **2013**, 42, 12020.
- (23) (a) Taylor, R. P.; Templeton, D. H.; Zalkin, A.; Horrocks, W. D. *Inorg. Chem.* **1968**, 7, 2629. (b) Alyea, E. C.; Costin, A.; Ferguson, G.; Fey, G. T.; Goel, R. G.; Restivo, R. J. *J. Chem. Soc., Dalton Trans.* **1975**, 1294. (c) Wolf, J.; Labande, A.; Natella, M.; Daran, J.-C.; Poli, R. *J. Mol. Catal. A: Chem.* **2006**, 259, 205. (d) Wolf, J.; Labande, A.; Daran, J.-C.; Poli, R. *J. Organomet. Chem.* **2006**, 691, 433. (e) Gwynne, E. A.; Stephan, D. W. *Organometallics* **2011**, 30, 4128. (f) Fischer, P.; Linder, T.; Radius, U. Z. *Anorg. Allg. Chem.* **2012**, 638, 1491. (g) Xu, Y.-C.; Zhang, J.; Sun, H.-M.; Shen, Q.; Zhang, Y. *Dalton Trans.* **2013**, 42, 8437. (h) Poppel, T.; Hinz, A.; Köckerling, M. *Polyhedron* **2013**, 52, 482.
- (24) Henrion, M.; Oertel, A. M.; Ritleng, V.; Chetcuti, M. J. *Chem. Commun.* **2013**, 49, 6424.
- (25) (a) Arnold, P. L.; Rodden, M.; Davis, K. M.; Scarisbrick, A. C.; Blake, A. J.; Wilson, C. *Chem. Commun.* **2004**, 1612. (b) Zhao, D.; Fei, Z.; Scopelliti, R.; Dyson, P. J. *Inorg. Chem.* **2004**, 43, 2197. (c) Ray, L.; Katiyar, V.; Raihan, M. J.; Nanavati, H.; Shaikh, M. M.; Ghosh, P. *Eur. J. Inorg. Chem.* **2006**, 3724.
- (26) (a) Garrison, J. C.; Youngs, W. J. *Chem. Rev.* **2005**, 105, 3978. (b) Haque, R. A.; Nasri, S. F.; Iqbal, M. A. *J. Coord. Chem.* **2013**, 66, 2679. (c) Kriechbaum, M.; Höbling, J.; Stammer, H.-G.; List, M.; Berger, R. J. F.; Monkowius, U. *Organometallics* **2013**, 32, 2876.
- (27) (a) Newman, C. P.; Clarkson, G. J.; Rourke, J. P. *J. Organomet. Chem.* **2007**, 692, 4962. (b) Su, H.-L.; Pérez, L. M.; Lee, S.-J.; Reibenspies, J. H.; Bazzi, H. S.; Bergbreiter, D. E. *Organometallics* **2012**, 31, 4063. (c) Topf, C.; Leitner, S.; Monkowius, U. *Acta Crystallogr. E* **2012**, 68, m272.
- (28) Fliedel, C.; Schnee, G.; Braunstein, P. *Dalton Trans.* **2009**, 2474.
- (29) Fliedel, C.; Braunstein, P. *Organometallics* **2010**, 29, 5614.
- (30) Chessa, S.; Clayden, N. J.; Bochmann, M.; Wright, J. A. *Chem. Commun.* **2009**, 797.
- (31) (a) Herrmann, W. A.; Gerstberger, G.; Spiegler, M. *Organometallics* **1997**, 16, 2209. (b) McGuinness, D. S.; Cavell, K. J.; Skelton, B. W.; White, A. H. *Organometallics* **1999**, 18, 1596. (c) McGuinness, D. S.; Mueller, W.; Wasserscheid, P.; Cavell, K. J.; Skelton, B. W.; White, A. H.; Englert, U. *Organometallics* **2002**, 21, 175. (d) Berding, J.; van Paridon, J. A.; van Rixel, V. H. S.; Bouwman, E. *Eur. J. Inorg. Chem.* **2011**, 2450.
- (32) (a) Hahn, E. F.; Heidrich, B.; Hepp, A.; Pape, T. *J. Organomet. Chem.* **2007**, 692, 4630. (b) Berding, J.; Lutz, M.; Spek, A. L.; Bouwman, E. *Appl. Organomet. Chem.* **2011**, 25, 76.
- (33) (a) Winston, S.; Stylianides, N.; Tulloch, A. A. D.; Wright, J. A.; Danopoulos, A. A. *Polyhedron* **2004**, 23, 2813. (b) Ketz, B. E.; Ottenwaelder, X. G.; Waymouth, R. M. *Chem. Commun.* **2005**, 5693. (c) Waltman, A. W.; Ritter, T.; Grubbs, R. H. *Organometallics* **2006**, 25, 4238.
- (34) (a) Li, W.-F.; Sun, H.-M.; Wang, Z.-G.; Chen, M.-Z.; Shen, Q.; Zhang, Y. *J. Organomet. Chem.* **2005**, 690, 6227. (b) Lee, C. C.; Ke, W. C.; Chan, K. T.; Lai, C. L.; Hu, C. H.; Lee, H. *Chem.—Eur. J.* **2007**, 13, 582. (c) Chen, C.; Qiu, H.; Chen, W.; Wang, D. *J. Organomet. Chem.* **2008**, 693, 3273. (d) Zhang, X.; Liu, B.; Liu, A.; Xie, W.; Chen, W. *Organometallics* **2009**, 28, 1336.
- (35) (a) Houghton, J.; Dyson, G.; Douthwaite, R. E.; Whitwood, A. C.; Kariuki, B. M. *Dalton Trans.* **2007**, 3065. (b) Huynh, H. V.; Yuan, D.; Han, Y. *Dalton Trans.* **2009**, 7262. (c) Warsink, S.; de Boer, S. Y.; Jongens, L. M.; Fu, C.-F.; Liu, S.-T.; Chen, J.-T.; Lutz, M.; Spek, A. L.;

Elsevier, C. J. *Dalton Trans.* **2009**, 7080. (d) Yuan, D.; Huynh, H. V. *Organometallics* **2010**, 29, 6020. (e) Yuan, D.; Tang, H.; Xiao, L.; Huynh, H. V. *Dalton Trans.* **2011**, 40, 8788. (f) Yuan, D.; Huynh, H. V. *Dalton Trans.* **2011**, 40, 11698.

(36) (a) Càmpora, J.; Ortiz de la Tabla, L.; Palma, P.; Alvarez, E.; Lahoz, F.; Mereiter, K. *Organometallics* **2006**, 25, 3314. (b) Zhang, X.; Liu, B.; Liu, A.; Xie, W.; Chen, W. *Organometallics* **2009**, 28, 1336.

(37) Jothibasur, R.; Huang, K.-W.; Huynh, H. V. *Organometallics* **2010**, 29, 3746.

(38) (a) Brown, D. H.; Skelton, B. W. *Dalton Trans.* **2011**, 40, 8849. (b) MaGee, K. D. M.; Travers, G.; Skelton, B. W.; Massi, M.; Payne, A. D.; Brown, D. H. *Aust. J. Chem.* **2012**, 65, 823.

(39) Liao, C.-Y.; Chan, K.-T.; Chang, Y.-C.; Chen, C.-Y.; Tu, C.-Y.; Hu, C.-H.; Lee, H. M. *Organometallics* **2007**, 26, 5826.

(40) (a) Shibata, T.; Ito, S.; Doe, M.; Tanaka, R.; Hashimoto, H.; Kinoshita, I.; Yano, S.; Nishioka, T. *Dalton Trans.* **2011**, 40, 6778. (b) Bernhammer, J. C.; Huynh, H. V. *Organometallics* **2014**, DOI: 10.1021/om500484q.

(41) (a) Huynh, H. V.; Wu, J. J. *Organomet. Chem.* **2009**, 694, 323. (b) Teng, Q.; Upmann, D.; Ng Wijaya, S. A. Z.; Huynh, H. V. *Organometallics* **2014**, 33, 3373.

(42) (a) O'Reilly, M.; Pattacini, R.; Braunstein, P. *Dalton Trans.* **2009**, 6092. (b) Bergem, N.; Blindheim, U.; Onsager, O. T.; Wang, H. Fr. Patent 1519181, 1968.

(43) Svejda, S. A.; Brookhart, M. *Organometallics* **1999**, 18, 65.

(44) (a) Errington, R. J. *Advanced Practical Inorganic and Metalorganic Chemistry*; CRC Press: Boca Raton, FL, 1997;. (b) Liu, J.; Chen, J.; Zhao, J.; Zhao, Y.; Li, L.; Zhang, H. *Synthesis* **2003**, 2661. (c) *Synthesis of Organometallic Compounds*; Komiyama, S., Ed.; Wiley: Chichester, 1997; Chapter 12.

(45) Williams, D. B. G.; Lawton, M. J. *Org. Chem.* **2010**, 75, 8351.

(46) Sheldrick, G. M. *Acta Crystallogr. A* **2008**, 64, 112.